INVESTIGATING THE BIOGEOBATTERY MODEL FOR FIELD SPONTANEOUS POTENTIAL (SP) SIGNATURES OVER AN ORGANIC RICH PLUME AT THE NORMAN LANDFILL, OK

By

SEN WEI

Bachelor of Science

LIAONING TECHNICAL UNIVERSITY

FUXIN, LIAONING,CHINA

2009

Submitted to the Faculty of the
Graduate College of the
Oklahoma State University
In partial fulfillment of
The requirements for
The Degree of
MASTER OF SCIENCE
December, 2012

INVESTIGATING THE BIOGEOBATTERY MODEL FOR FIELD SPONTANEOUS POTENTIAL (SP) SIGNATURES OVER AN ORGANIC RICH PLUME AT THE NORMAN LANDFILL, OK

Thesis Approved:

Dr. Estella Atekwana

Thesis Adviser

Dr. Eliot Atekwana

Dr. Priyank Jaiswal

Dr. Todd Halihan

ACKNOWLEDGEMENTS

I am heartily thankful to Dr. Estella Atekwana, my advisor, for her patience in dealing with my stubbornness, her encouragement and support throughout the work on this project and mostly for allowing me to work independently. She has supported me in many ways including support for data acquisition, access to software, and equipment used for this study.

Furthermore, I wish to thank Dr. Eliot Atekwana, Dr. Todd Halihan and Dr. Priyank Jaiswal for serving on my committee and for their valuable contributions in making this work better.

Appreciation is extended to Dr. G.Z. Abdel Aal for his help with the fieldwork, experiment and suggestions. In addition, I would like to thank Jason Masoner and Kevin Smith from the U.S Geological Survey for giving me access to valuable geochemical data and their support in the field.

Also I would like to thank my friends: Eric Akoko, Jon Sanford, Farag Mewafy and Byron Waltman for help with fieldwork.

Finally, I offer special thanks to my parents for their love and support and who supported me financially and made my studies in the USA possible. Partial funding for this project was provided by Chevron Energy Technology Company.

Acknowledgements reflect the views of the author and are not endorsed by committee members or Oklahoma State University.

Name: SEN WEI

Date of Degree: DECEMBER, 2012

Title of Study: INVESTIGATING THE BIOGEOBATTERY MODEL FOR FIELD SPONTANEOUS POTENTIAL (SP) SIGNATURES OVER AN ORGANIC RICH PLUME AT THE NORMAN LANDFILL, OK

Major Field: GEOLOGY

Abstract: A Self Potential (SP) survey was conducted over the leachate plume emanating from the Norman Landfill site in Norman, OK. Investigating the source mechanism of SP signatures will improve geophysical imaging techniques for non-invasive and sustainable monitoring of plume conditions within urban landfill sites. Recent studies have suggested a strong correlation between SP anomalies and microbial driven redox processes recorded at landfill sites. These studies suggest that strong current sources (biogeobatteries) are generated at the sharp redox boundary occurring at the water table interface where biofilms and metallic biominerals can facilitate electron transfer between reduced and oxidized zones. However this biogeobattery model is highly debatable since so far only one studyhas documented its validity at organic rich contaminated sites. Therefore the objectives of this study include: 1). acquire SP, electrical resistivity (ER) data across the landfill leachate plume; 2). use existing geochemical data to verify the occurrence of active biodegradataion and the terminal electron acceptor processes; 3). determine the existence of bio-induced metallic minerals that may serve as conductors that facilitate electron transport from reduced (below the water table) to oxidized zones above the water table and 4). confirm or refute the existence of the biogeobattery model at the Norman Landfil as a driving mechanism for the SP anomalies.

SP measurements, electrical resistivity (ER) survey, geochemical data and borehole magnetic susceptibility measurements were made. Small SP anomalies (ranging from 9 to -12 mV) were obtained over the landfill leachate plume; electrical resistivity data was able to delineate the leachate plume (ranging from 5~15 ohm.m). In addition, a high magnetic susceptibility (increase from 0.004 to 0.009 SI unit) layer was found existing just below the water table interface. Although the magnetic susceptibility data suggests the presence of metallic biominerals (greigite) capable of moving electrons across the water table interface bridging anaerobic and aerobic environments, the small SP anomalies negates the existence of a bio-geobattery as a source of the SP anomalies. Instead the SP anomalies can be simply explained as resulting from diffusion potentials.

TABLE OF CONTENTS

LIST OF FIGURES

LIST OF TABLE

CHAPTER I

INTRODUCTION

1.1 Problem statement

Spontaneous Potential (also called self-potential, SP) is one of the oldest and cheapest geophysical techniques that have been widely used in the mineral exploration for detecting massive sulfide deposits as these deposits generally generate potentials in hundreds of millivolts. Such mineralization potentials have been adequately explained with the classic geobattery model (Figure 1.1 (a)) provided by Sato and Mooney (1960). A large SP signal is observed over ore deposits and generated from geochemical redox reactions with the metallic body serving as an electronic conductor transferring electrons from reduced zones to oxidized zones, behaving as a geobattery.

Recently, the SP method has been successfully applied to a variety of environmental field investigations to detect/approximate water table elevation (e.g., Sailhac and Marquis 2001; Darnet et al., 2003), delineation of preferential water flow pathways (e.g., Bogoslovsky and Ogilvy 1970; Song et al. 2005), and investigation of contaminant plumes (e.g., Che-Alota et al., 2009; Arora et al., 2007; Naudet et al., 2003; 2004; Sauck et al., 1998). In addition, there is increasing interest in SP to detect and monitor subsurface microbial processes (e.g., Nyquist and Cory, 2005; Slater et al., 2007; Arora et al., 2007; Ntarlagiannis et al., 2007; Che-Alota et al., 2009; Forté, 2011). Although the geobattery model describing SP mechanisms over ore bodies is generally accepted, the

source mechanisms of SP anomalies due to electrochemical potentials observed over organic contaminant sites mitigated by microbial activityremain speculative and highly debatable (Natlargiannis et al., 2007; Revil et al., 2010). For example, Naudet et al. (2004; 2005) and Aurora et al. (2007) documented a strong relationship between SP signals and redox potential (Eh) measurements and suggested that SP can be used to non-intrusively derive Eh.In the Naudet et al. (2004) study, the authors documented strong SP anomalies (up to -400 mv) at the Entressen landfill in Southern France and correlated the SP anomalies to microbe driven redox reactions. Arora et al. (2007) proposed a geobattery model associated with the biodegradation of organic rich plumes to explain the Naudet et al.(2004) results.In this model a natural battery exists across the water table boundary, separating highly reduced, oxygen depleted areas within the plume and oxygen-rich conditions surrounding the contaminant plume. In order to complete the geobattery circuit, Arora et al. (2007) hypothesized that the presence of biomass/biofilms and metallic mineral precipitates serve as electron conductors and the redox gradient is attributed to the concentration of dissolved Fe2+ due to oxidation of organic matter (Figure 1.1 (b)). As a matter of fact, this is the only field evidence that has recorded such large negative SP anomalies that are microbially driven. Che-Alota et al. (2009) recorded small SP anomalies over a hydrocarbon contaminated undergoing biodegradation although strong redox gradients occurred at the site. Large SP anomalies have been documented in the laboratory (Ntarlagiannis et al., 2007; Williams et al., 2007), however the sources of these anomalies are highly debatable. In the Ntarlagiannis et al. (2007) study, they related their response to electric current sources resulting from the production of microbial nanowires that have been suggested to transport electrons from microbial

cells to distant electron acceptors (Gorby et al., 2006; Ruguera et al., 2005). However, Williams et al. (2007) suggested that such large SP anomalies may have resulted from reactions between electrodes and metabolic byproducts, in which case the term electrodic potentials is more appropriate. Castermant et al. (2008) demonstrated through a laboratory experiment that large redox gradients are not sufficient to generate large SP anomalies and that an electronic conductor is needed as suggested in the model presented in Figure 1.2. More recently, Forté (2011) documented very small SP anomalies from two hydrocarbon contaminated sites and concluded that the SP response could not be explained by a geobattery model.

Revil et al. (2010) has proposed the conditions conducive for the occurrence of a biogeotattery.Bio-geobatteries may occur in conjunction with a strong redox gradient between highly reducing conditions below the water table within a contaminant plume and an oxidized zone above the water table if microbial activity can generate the required electron bridge (Revil et al., 2010).Possible mechanisms facilitating electron migration include iron oxides, clays, and conductive biological materials (Revil et al., 2010). Metal reducing organisms, such as Shewanella and Geobacter, produce electrically conductive appendages called bacterial nanowires that may facilitate electron transfer to solid phase electron acceptors (Gorby et al., 2006, Reguera, 2005). However, the ability of biofilms to facilitate electron transport over the scale of the groundwater interface is unknown although new evidence suggests that such electron transfer at least can take place at mm scales resulting in the electrical coupling of biogeochemical processes in spatially separated regions (Nielsen et al., 2010; Risgaard-Petersen et al., 2012). In addition a recent study by Kato et al. (2012) suggest that microorgasims can utilize conductive

minerals such as magnetite as conduits for electron transfer resulting in efficient inter species electron transfer contributing to the coupling of different biogeochemical reactions. Field studies at organic rich contaminated sites undergoing biodegradation are needed to confirm this exciting new finding.

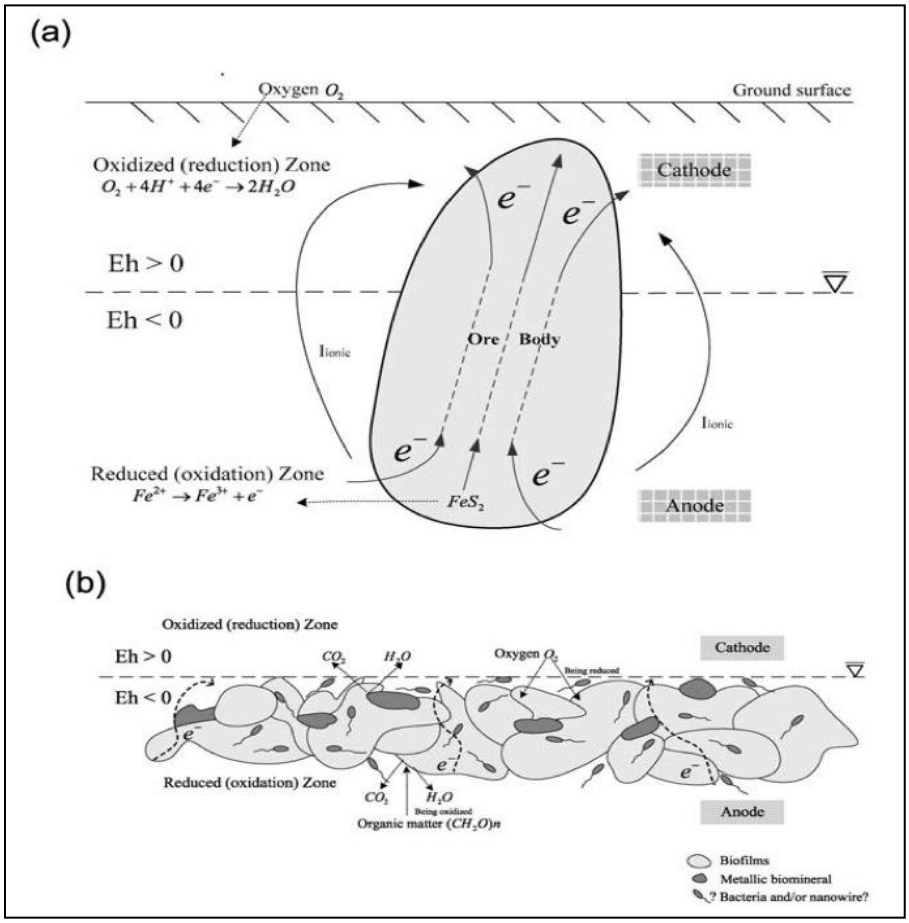

Figure 1.1 (a) The Sato and Mooney (1960) geobattery model where the redox gradient is attributed to the gradient of dissolved oxygen in groundwater and the ore body serves as the electron conductor (from Castermant et al. (2008), Revil et al.(2010)) and (b) the biogeobattery model proposed by Naudet et al. (2004) where the redox gradient is attributed to the gradient in dissolved Fe^{2+} resulting from oxidation of organic matter, biofilms and biominerals at the water table serve as the electron conductor.

Recently studies by Mewafy et al. (2011) have documented the presence of a magnetite enriched layer within the smear zone, straddling the water table at a hydrocarbon contaminated site due to microbial iron reduction coupled to hydrocarbon oxidation.

Does the bio-metallic mineral layer detected at the water table represent the "missing" electronic conductor needed to transfer electrons from the anode (below the water table) to the cathode (above the water table) generating large SP anomalies?

In this study I extend the work of Naudet et al. (2004) and Mewafy et al. (2011) to investigate SP anomalies over the Norman Landfill.

1.2 Objectives

The overall goal of this study is to understand the processes generating SP anomalies and confirm or refute the biogeobattery model at the Norman landfill site. Specific questions to be answered: 1). What is the magnitude of the SP signals associated with the Norman landfill plume? 2). Does a bio-metallic enriched layer exist across the water table interface? 3). Is there a relationship between SP and Eh as documented over the Entressen landfill? 4). What is the source mechanism generating the SP response and does a bio-geobattery exist over the Norman landfill plume?

1.3 Contributions of this work

The self-potential study on Norman Landfill site with organic-rich contaminated plumes in groundwater provides a field test for the biogeobattery model of Revil et al. (2010). The results suggest that although a magnetic enriched layer exists above the water table interface, the SP anomalies observed are too small to result from a geobattery at depth. This research proposes that within organic-rich contaminated sites, the source of SP anomalies is generated by the coupling of redox potentials and diffusion potentials that are largely driven by microbial activities.

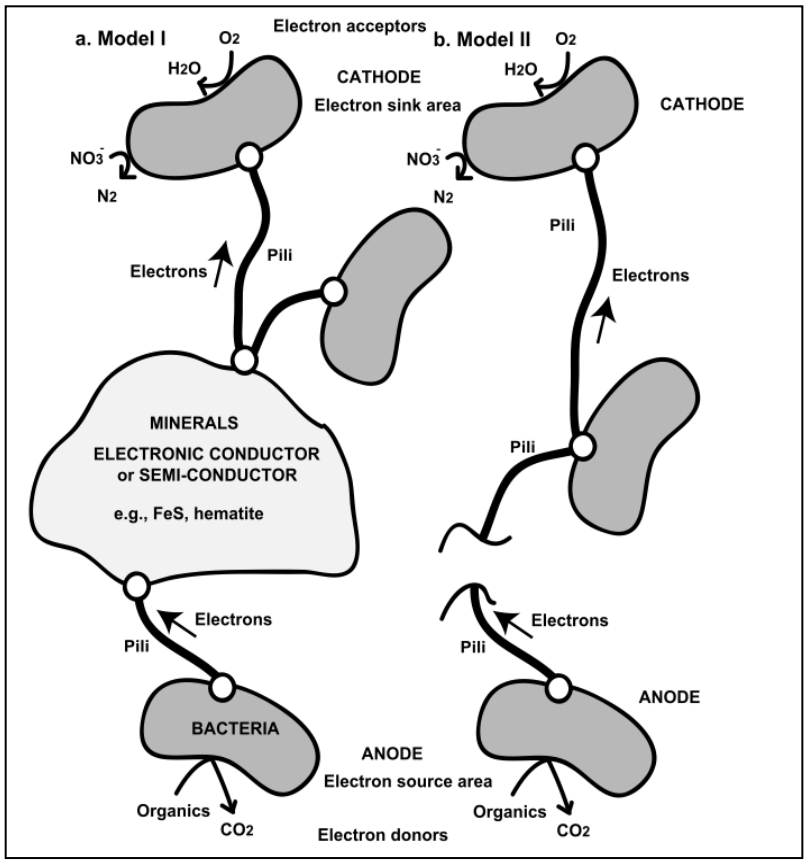

Figure 1.2 Biogeobattery models supported by Revil at al. 2010. (a) In model I, the presence of minerals linked to bacteria through extracellular appendages (pili) facilitates electronic conduction. (b) In model II, only bacteria populations are connected by conductive pili. At the ‘‘bacterial anode,’’ electrons are gained through the oxidation of the organic matter, iron oxides, or Fe-bearing phyllosilicates. The electrons are conveyed to the ‘‘bacterial cathode’’ through a network of conductive pili. At the ‘‘bacterial cathode,’’ the reduction of oxygen and the nitrate prevails as electron acceptors. In this system, bacteria act as catalysts. The transport of electrons through the anode to the cathode of the microbattery may involve different bacterial communities (inter species electron transfer) and different electron transfer mechanisms including external electron shuttles.

1.4 Layout of thesis

Chapter 2 includes the site history, geologic and geochemical settings that describe the background of the Norman Landfill Site. The literature review is presented in chapter 3 and introduces past and present studies on explaination of SP source mechanisms. Theoretical methods including SP, electrical resistivity, magnetic method and

geochemical method are introduced in chapter 4 that are applied in the research. In chapter 5 detailed descriptions of geophysical (SP, ER and Magnetic Susceptibility) and geochemical data collection and processing are presented.Results are presented in chapter 6. Conclusions and suggestions for future work are presented in chapter 7.

CHAPTER II

SITE DESCRIPTION

2.1 Site History

The Norman Landfill has been identified as a source of dissolved organic and inorganic compounds in ground water (Beeman and Suflita, 1987; Beeman and Suflita, 1990). This closed municipal solid waste landfill is located in the south of Norman, OK near the Canadian River (Figure 2.1). This landfill operated from 1922 to 1985 and is a typical unlined landfill in an alluvial aquifer. The landfill started as an open dump in the early 1900s, however there were no restrictions about the types of the waste. According to the closure report by Dixon (1992), the waste is mainly residential and commercial solid waste, as well some suspected hazardous waste disposal. The capped landfill consists of an asphalt plant and two cells: east cell and west cell (Figure 2.1). The landfill therefore produces leachate containing many organic compounds found in consumer products such as pharmaceuticals, plasticizers, disinfectants, cleaning agents, fire retardants, flavorings, and preservatives, known as emerging contaminants (ECs) (Andrews et al., 2012). Ground water at this site is contaminated by organic compounds, many of which are toxic and carcinogenic. Geochemical and microbial data suggest that biodegradation of the organic plume is occurring in the well-characterized redox zone. Thus, this site could be regarded as an ideal site for investigation of SP anomalies resulting from biological

activity.Geophysical and geochemical measurements have shown that a leachate plume extends southwest from the landfill toward the Canadian River (Schlottmann, 2001).

The Norman Landfill was selected for study as part of the U.S. Geological Survey (USGS) and Water Resources Division (WRD) Toxic Substances Hydrology Program (TSHP) in 1994, since it offers unique opportunities for scientific research in an exceptionally dynamic hydrologic system. The hydrology near the Norman Landfill includes dynamic interactions between ground water and surface water (both natural and anthropogenic), complex permeability structure in alithologically heterogeneous aquifer, the processes of attenuation and degradation for the contaminants and the geochemical reaction in a groundwater environment (Cozzarelli et al., 2000).

Lucius and Bisdorf (1995) delineated the vertical and horizontal extent of the leachate plume by using electromagnetic (EM) induction, Direct current (DC) resistivity and ground penetrating (GPR) methods. Schlottmann (1995) described initial investigations of the ground and surface water chemistry that indicated the presence of leachate in the ground water. Cogoini (1997) described the soil magnetic properties at the landfill and suggested that magnetite exists in the plume area which caused magnetic susceptibility (MS) variations. In recent years, scientists are focusing on the changes in the source of contamination and biogeochemical processes over time as reactions at these sites progress, because the fate of organic contaminants depends on geochemical reactions in the subsurface that are most often microbially mediated (Cozzarelli et al., 2010).

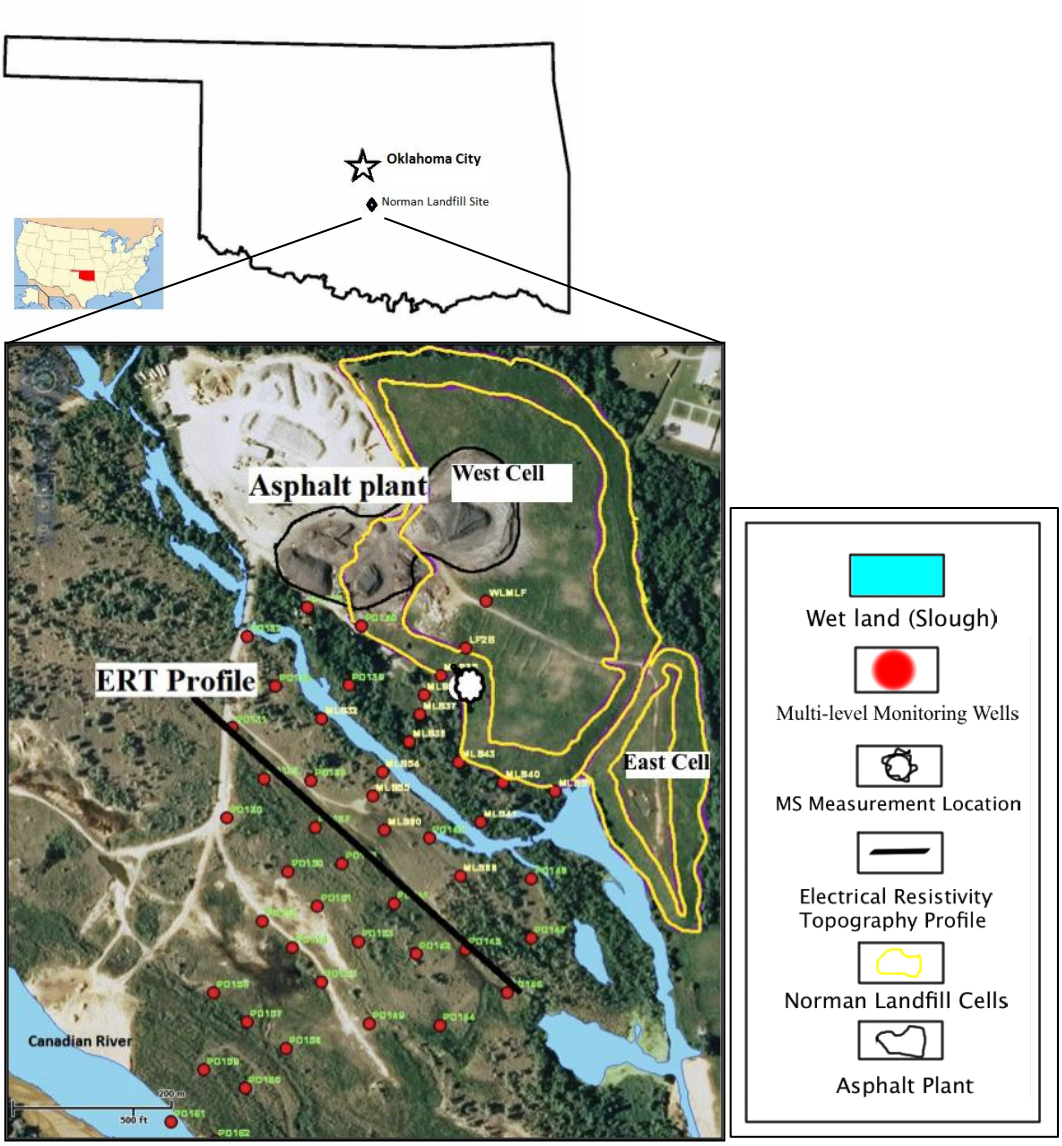

Figure 2.1 Map of the Norman Landfill site showing locations of Norman Landfill cells, multi-level monitoring wells, Magnetic Susceptibility (MS) measurement location, electrical resistivity tomography profile, asphalt plant location, slough and Canadian River (modified from USGS, http://sitios.csa.ou.edu/landfill/flexviewer231/bin-debug/)

2.2 Geologic Setting

In 1985, the base of the Norman Landfill area covered about 314,000 m2 and its capped area was 186000 m2. The weight of buried waste is about 2.6 million tons and the cap is 12 to 15 meters high above the surrounding alluvium (Becker, 2002). The Canadian River alluvium, Quaternary in age, is predominantly of interbedded, discontinuous layers

of red-brown clayey silt and gravel with a pale red, fine-to medium-grained sand bed that is about 10 to 12 meter thick (Callender et al.,1993). Beneath the alluvium there is the Hennessey Group of Permian age shale and siltstone with a low permeability acting as the lower boundary. The Garber Sandstone also Permian in age, lies below the Hennessey Group and consists of lenticular beds of fine-grained, massive-appearing, cross-bedded sandstone irregularly interbedded with shale, siltstone and mudstone (Wood and Burton, 1968; Parkhust et al., 1993). Between the Garber sandstone and the Hennessey Group is the contact that has been documented as apparently conformable and there may be a zone up to 10 m thick where the two formations interfinger (Wood and Burton, 1968). At the elevation of 319 m, a high conductive layer consisting of gravel and coarse sand locates at the base of the alluvium. Above the alluvium a discontinuous low conductivity interval consisting of silt and clay is found at the elevation between 326 and 328 m in the plume leachate area.

2.3 Biogeochemical Processes at the Norman Landfill

The Canadian River is located about 600 m southwest from the landfill (Figure. 2.1). The river flows southeast and is separated from the landfill by a flat area characterized by thick vegetation such as trees, native grasses and shrubs. Affected by the rainfall and seasonal evapotranspiration, the water table in the Canadian River alluvium fluctuates less than 2 m in the landfill (Scholl et al., 2004). It is stated that differences in magnitude of seasonal variations in water levels affect biogeochemical reactions rates at the interface between leachate and overlying recharge water (Cozzarelli et al., 2011). There is a shallow stream (about 100 m from the edge of the landfill) caused by beaver dams

(referred to as slough) flowing from the northwest to the southeast which has an average depth about 0.75 m.

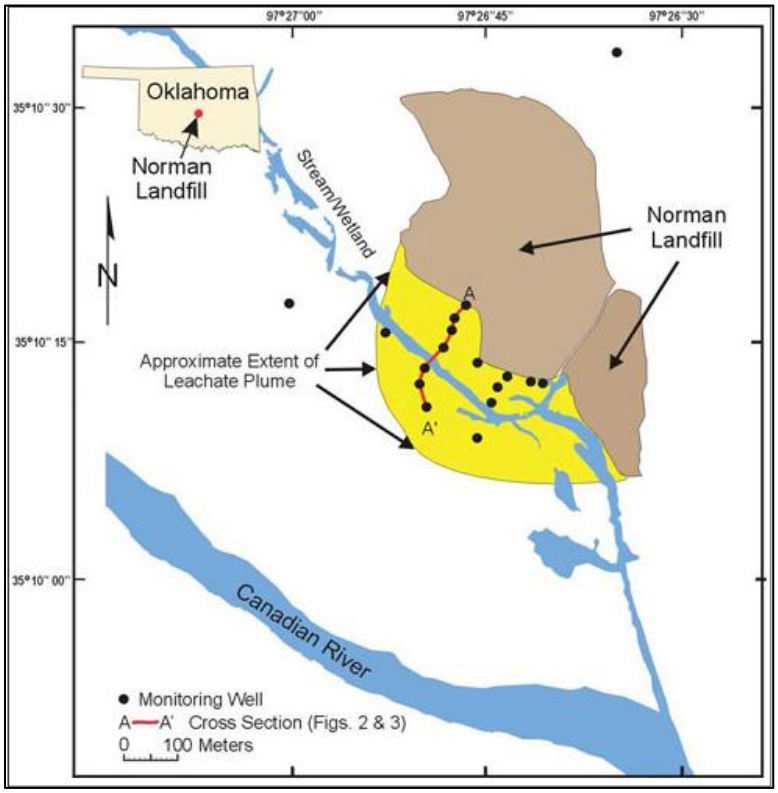

Figure 2.2 Approximate extent of leachate plume (yellow) (Scott and Cozzarelli,2003).

The plume area (Figure 2.2) was delineated by geochemical data from multilevel monitoring wells (Scott and Cozzarelli, 2003). Cozzarelli et al. (2011) described the hydrologic model (Figure 2.3) of the leachate plume in the alluvial aquifer downgradient from the Norman Landfill. Cozzarelli et al. (2000) summarized the integrated geochemical and microbiological approach in Table 2.1, and provided a comprehensive picture of biogeochemical processes in the contaminated aquifer.

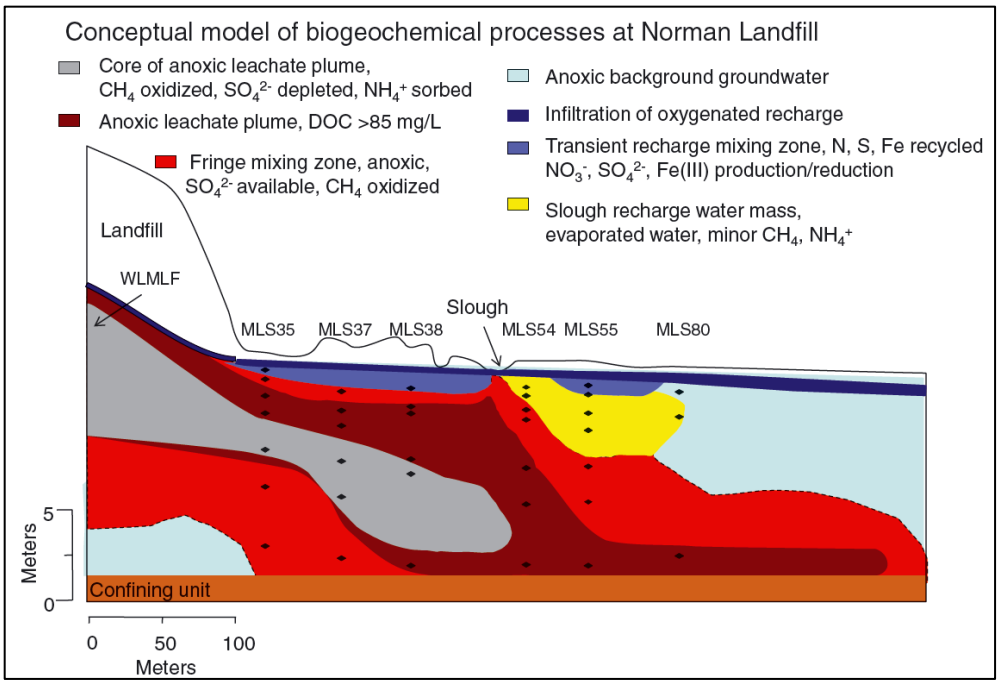

Figure 2.3 Model of the important hydrologic and geochemical features of the leachate plume in the alluvial aquifer. (Cozzarelli et al., 2011)

The oxidation of organic matter corresponds with reduction reactions such as oxygen to water, nitrite to elementary nitrogen N2, manganese (III / IV) to manganese (II), iron (III) to iron (II), sulphate to sulphide and CO2 to methane (Cozzarelli et al., 2011). Microbial activity is essential in redox processes since microbes derive energy from oxide-reduction reactions to maintain life-sustaining processes (Chriestensen et al., 2000).

Table 2.1 Indicators of Active Terminal Electron-Accepting Processes (TEAP)

TEAP	**Electron acceptor concentration decrease**	**Reduced products increase**	**Microbial activity present (microcosms)**	**H^+ concentration (nM)**
CO_2 reduction	CO_2	CH_4	Methane	>4.0

			production	
SO_4^{2-} reduction	SO_4^{2-}	H_2S	Sulfate reduction	1.0-4.0
F_e^{3+} reduction	Solid-phase (FeIII)	F_e^{2+}	Iron reduction	0.1-0.8
NO_3^- reduction	NO_3^-	NH_4^+	Nitrate reduction	<0.10

Terminal electron acceptor processes by bacteria for degrading the landfill organic matters are identified as SO_4^{2-} and Fe3+ minerals (Kennedy and Everet, 2001). It has been documented that sulfate reduction is the dominant terminal electron accepting process occurring at this site (Cozzarelli et al., 1996). The direct enzymatic reduction of F_e^{3+} minerals may produce a certain amount of dissolved F_e^{2+} as:

$$CH_2O + 4Fe^{3+}_{(s)} + H_2O \rightarrow 4Fe^{2+}_{(aq)} + CO_2 + 4H^+ \quad (2.1)$$

A general equation for sulfate reduction can be written as:

$$CH_2O + \frac{1}{2}SO_4^{2-} \rightarrow \frac{1}{2}HS^-_{(aq)} + HCO_3^- + \frac{1}{2}H^+ \quad (2.2)$$

The leachate plume is characterized and delineated by high values of chloride concentrations, the electrical conductivity of the water and elevated concentrations of nonvolatile dissolved organic carbon (NVDOC) (up to 300 mg/L), methane (16 mg/L), ammonium (650 mg/L as N), iron (23 mg/L), chloride (1030 mg/L), and bicarbonate (4270 mg/L).

CHAPTER III

LITERATURE REVIEW

Over the last two decades, the application of SP to contaminant plume mapping has been on the rise. The debate started with the Naudet et al. (2004) paper which stated that the SP signals detected in the landfill is associated with biogeobatteries, large redox potentials (up to -240mV) are generated at water table and electrons are carried by biominerals in the vadose zone; however this is the only paper recording such large SP anomalies at a landfill site. Ata hydrocarbon contaminated sites SP data both in borehole and at the surface were collected and significant changes were found at different times of the year due to the groundwater flow and oxidation-reduction phenomena due to bacterial activity (Giampaolo et al., 2012). They stated that SP anomaly variations with time are caused by bacterial activity where water table plays an important role.

Nevertheless, there is no consensus as to the source mechanism generating these SP anomalies. Corry (1985) and Nyquist and Corry (2002) suggested that the difference in redox potential between two measurement points is the source of SP anomalies. Ntarlagiannis et al. (2007) in a column experiment observed strong SP anomalies (>100mV) associated with microbial activity and stated that the electrons migrate through bacteria conductive pili, generating a current between domains of different redox potential. In contrast, Williams et al. (2007) proposed a different idea that there is

insufficient current flowing through biofilms to produce SP signals. Forté (2011) conducted SP surveys over two hydrocarbon contaminated sites and implied that there is no correlation between SP and electrokinetic or electrochemical sources. She proposed that the current sources of SP anomalies can be explained by two theoretical models: the diffusion model and Eh model. Forté (2011) applied a diffusion model that is calculated by using toluene biodegradation simulation data to explain small SP anomalies (ranging from 21 to -17 and 65 to -85mV respectively) at two sites. At a transition zone that is less resistive than background, the Eh model is essential to be applied in order to produce large SP anomalies with tested models. In contrast, Linde and Revil (2007) established a relationship between the self-potential and redox potential over the contaminant plume of the Entressen landfill, and suggested indirectly the potential role of microbial activity in transferring electrons through sharp redox potential gradient in organic matter contaminated plumes (Revil et al. 2009). Castermant et al. (2008) carried out a controlled sandbox experiment in the laboratory to investigate relationships between SP anomalies and redox potential. They stated that currents inside the iron bar are due to redox reactions and SP anomaly is therefore produced. Hence a biogeobattery (Figure 3.1) is further developed to explain and predict the change in magnitude and polarity of SP along a borehole in an oil spill contamination site (Revil et al., 2010).

The model correlates SP anomalies with electronic conductors which can control the magnitude of SP anomalies. They proposed that with enough electronic acceptors and donors, large SP anomalies (larger than 100mV) are generated only in the presence of abundant conductors. There is evidence stating that biofilms, nanowires and metals can serve as the electron conductors. Reguera et al. (2005) and Gorby et al. (2006) defined

"nanowire" as the term to describe external pili of bacteria used for transferring electrons. Ntarlagiannis et al. (2007) attribute SP anomalies to the electron donor availability and the nanowire building process. Although pili play an important role in electron transfer through the whole biofilm, electronic conduction through these nanowires has not been thoroughly studied (Atekwana and Slater, 2009).

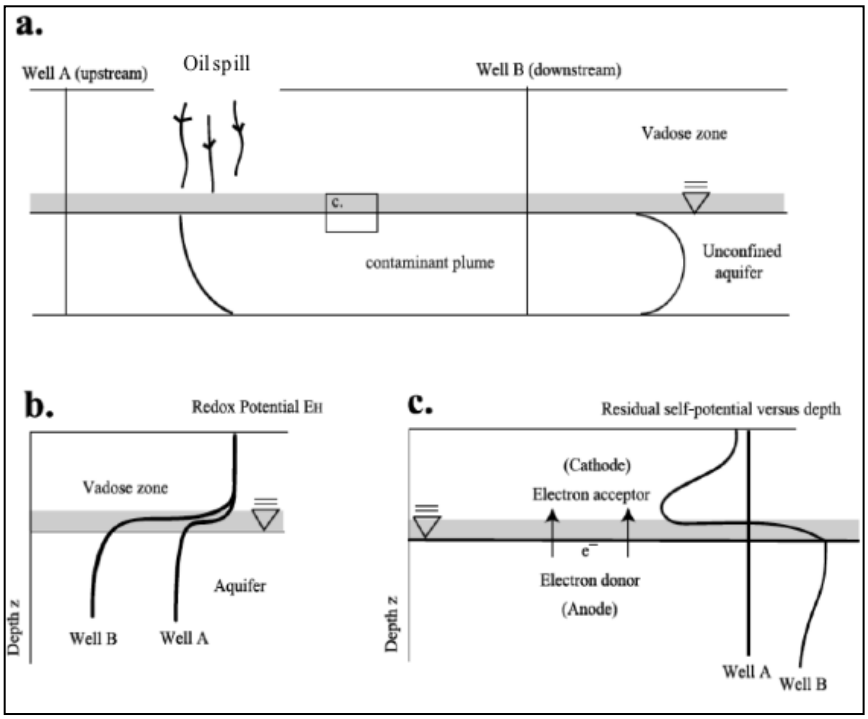

Figure 3.1 Sketch of the geobattery associated with an oil spill. (a) The oil spill results in a contaminant plume in an unconfined aquifer. (b) There is a stronger gradient of the redox potential through the capillary fringe (the gray area) above the contaminant plume by comparison with the profile shown upstream. (c) The capillary fringe of the contaminated portion of the aquifer is potentially the setting of an electron transfer mechanism normal to the water table. This battery generates a dipolar self-potential field. This model predicts a change in the polarity of the residual self potential (the measured self-potential minus the contribution related to groundwater flow) through the capillary fringe (after Revil et al., 2010)

Recent Magnetic susceptibility on cores retrieved from hydrocarbon contaminated sites have identified a magnetite enriched layer in the hydrocarbon smear zone, straddling the water table (Rijal et al., 2010; 2012; Mewafy et al., 2011). This magnetite layer is suggested to result from the coupling of hydrocarbon oxidation with iron reduction. Iron

oxides such as magnetite and maghemite, along with iron sulfides such as pyrrhotite and greigite are the most common ferric (III) magnetic minerals existing in soils, sediments and rocks (Tarling 1983). Among these minerals, magnetite and greigite have the highest value of MS (Ellwood and Burkart, 1996); while hematite, goethite and several paramagnetic substances including some clay have minimal effect on MS measurements (Thompson and Oldfield, 1986). MS differences are considered as a result of variation in soil and sediment type, changes in magnetic grain size or magnetic phase present (Maher, 1998; Thompson and Oldfield, 1986). Hence it is proposed that the increase in MS values is caused by the precipitation of magnetic mineral phases associated with microbial activity (Cogoini 1997). Thus, the magnetic layer formed at the water table might serve as the electronic conductor as proposed by Revil et al. (2010). Nevertheless, none of the field research has linked SP and MS methods together to explain SP mechanisms under contaminated conditions. Hence, this thesis is also used to test the relationships between SP signals and electronic conductors to investigate the effectiveness of the metallic layer in transporting electrons at organic-rich contaminated sites.

CHAPTER IV

THEORETICAL BASIS OF THE GEOPHYSICAL METHODS

4.1 Introduction

Several geophysical techniques were used to investigate the plume at the Norman Landfill site including SP, magnetic susceptibility and electrical resistivity.

4.2 Self Potential

The SP technique is based upon the measurement of naturally occurring electric potentials attributed to current sources in the subsurface. SP are measured with non-polarizable electrodes in contact with the ground surface or down boreholes. Electrodes placed at the ground surface are connected via wire to a high impedance (>10 M Ohm) voltmeter, and the electric potential is measured. Several mechanisms have been suggested to explain the SP anomalies: mineralization, electrokinetic, electrochemical, redox, and thermoelectric potentials (e.g., Nyquist and Corry 2002).

4.3 Mineralization Potentials (Geobattery model)

Mineralization potential, as the term suggests, is SP anomalies resulting from mineral ore deposits and a result of redox reactions. It has been measured and explained at Earth's surface in mineral exploration since 1960 by Sato and Mooney (Figure1.1), reduction reactions near the surface and oxidation reactions at depth contribute to the generation of

current inside the deposit. For example, we consider the mechanism of corrosion of an ore body like pyrite FeS_2 (Figure 1.1 (a)). At the oxic/anoxic interface (typically at water table) SO_4^{2-} and Fe^{2+} are released coupled to the reduction of oxygen due to the reactions of S(-II) and S(0) in the pyrite. The ferrous iron therefore reacts, through advective, dispersive, and electromigration transport, with oxygen at the water table that affect the distribution of the redox potential in the vicinity of the ore body. This mechanism can be summarized by the following reactions. Below the water table at the surface of the ore body, the following half-reaction occurs, mechanisms can be described by the following reactions:

$$FeS_2 + 8H_2O = Fe^{2+} + 2SO_4^{2-} + 14e^- + 16H^+ \quad (4.1)$$

While at the cathode (possibly within the vadose zone), we have the following reactions:

$$14e^- + 3.5O_2 + 14H^+ = 7H_2O \quad (4.2)$$

$$4Fe^{2+} + O_2 + 4H^+ = 4Fe^{3+} + 2H_2O \quad (4.3)$$

$$4Fe^{3+} + 12H_2O = 4Fe(OH)_3 + 12H^+ \quad (4.4)$$

The ore body in this case would behave as a conductor transferring electrons released during reactions from depth to the oxic/anoxic interface (Bigalke and Grabner, 1997). Large negative SP signals (-400~-1500 mV) are observed (Corry 1985; Stoll et al. 1995; Mendoca, 2008) at the ground surface due to redox reactions from ore deposits from underground.

4.4 Streaming Potentials

Streaming potential is created when groundwater is driven by a gradient through a channel or porous media, the electrical response is studied as a consequence of piezometric head distribution (Rizzo et al., 2004). The model of this mechanism has been well established (Fitterman 1979; Ishido and Pritchett 1999; Revil and Leroy 2001; Revil et al., 2003; Maineult et al., 2006; Suski et al., 2006) and used for illustrating SP signals coupled with ground water flow (Naudet et al., 2004). Sill (1983) proposed a classical description of electrokinetic theory that the current density is related to pore fluid pressure gradients. Naudet et al. (2003;2004) and Naudet and Revil (2005) determined the streaming potential coefficient by the ratio of SP differences and hydraulic head differences. Hence an equation is expressed by Naudet et al., (2003):

$$C' = \frac{\varphi - \varphi_0}{h - h_0} \quad (4.5)$$

where φ (in mV) is self potential at measurement station where the hydraulic head is h (in meter). Parameters of φ_0 and h_0 are electric potential and piezometric head at SP base station (φ_0 =0mV). Parameter C' is defined as streaming potential coupling coefficient (in mV per meter). In the field, C' can be calculated as the formulation expressed below:

$$C' = \frac{\Delta V}{\Delta h} \quad (4.6)$$

where ΔV stands for the SP difference and $\Delta h$is the groundwater head difference. The streaming potential coupling coefficient can be used for calculating the electrical potential variation given a head difference. As a result, a residual SP map can be achieved and certain relationships can be further analyzed between SP and electrochemical origin.

4.5 Electrochemical Potentials

The electro-diffusion potentials arise from chemical potentials of the ionic charge carriers (Linde and Revil 2007). Electrolytic concentration varies at different locations in the field, resulting in differences in the mobility of anion and cations that result in potential differences.

4.5.1 Membrane Potential and Diffusion Potential

The diffusion potentials, also called liquid junction potentials, are electro-diffusional effects which arise from chemical potentials of the ionic charge carriers (Linde and Revil, 2007). Electrolytic concentration varies at different locations in the field, resulting in differences in the mobility of anion and cations that result in potential differences. For example, if NaCl solution is put into pure water, the Na+ and Cl- can diffuse into the pure water region due to the concentration gradient. However, because of the higher mobility of Cl- ions than that of Na+, Cl- ions can move into the region faster creating a charge separation that produces an electrical potential. Due to the function of the potential, the speed of Cl- ions will be reduced while Na+ ions can move faster and ultimately they can move at the same velocity though a separation remains (Keller and Frischknecht, 1996). Concentration difference of ions on opposite sides of a cellular membrane can create voltage named the membrane potential. In geologic context, the membrane could be the contact between sandstone and shale, as the shale is permeable to Na+ ions but not to Cl- ions (Nyquist and Corry, 2002). Timm and Moller (2001) proposed that in laboratory experiments membrane potential can be established since cations and anions are separated because of individual interactions between cations and mineral surfaces. The membrane potential is given by the equation:

$$\phi = \frac{RT}{F} \ln \frac{a1}{a2} \quad (4.7)$$

where a_1 and a_2 are ion activities in solution one and two, $\phi$is membrane potential, R is the universal gas constant (R = 8.314472 $J \cdot K^{-1} \cdot mol^{-1}$), T is the temperature and F is Faraday's constant (F = 96485.3383±0.008 C/mol) (Atkins, 1990).

Assume 1). Activity coefficients are taken as unity; 2). Transport numbers are constant and 3). A linear variation of concentration with distance, the diffusion potential yields the Plank-Henderson equation (Bockris and Reddy, 1998, eq.4.289):

$$\phi = \frac{RT}{F} \sum_i \frac{t_i}{z_i} \frac{c_i(l)}{c_i(0)} \quad (4.8)$$

where t_i and z_i are the transport number and valence of ion I and $c_i(0,l)$ are the concentrations of ion I at distances 0 and l. Both streaming and diffusion potentials can generate small potential anomalies in the tens of millivolts range in contrast to hundreds millivolts range from mineralization potentials.

The SP method is also widely used in the oil and gas industry for formation evaluation in boreholes. When oil leaks into shale above the reservoir, degradation happens which can form a reduction zone with respect to the surrounding oxidized sediment. Hence electric currents can be detected due to a redox galvanic cell (Pirson, 1981).

4.5.2 Redox Potential

The redox potential, also called oxidation-reduction reactions, is produced by the abundance of oxidized and reduced species. Under equilibrium conditions it is given by Nernst equation (Timm and Moller, 2001):

$$E_H = E_0 + \frac{RT}{zF} ln \frac{a_{ox}}{a_{red}} \quad (4.9)$$

where E_0 is the standard potential, R is the gas constant, T is the temperature. Z is the number of electrons transferred in the reaction formula; F is the Farady's constant (F = 96485.3383±0.008 C/mol), a_{ox} and a_{red} are the activity of the oxidized and reduced species respectively.

4.6 Resistivity

In electrical resistivity methods direct current (DC) or low-frequency alternating currents is applied at the ground surface, and the potential differences are measured between two points. Different types of layer have different resistance so that we can find useful information about the structure and materials the site contains. Figure 4.1 indicates the simple array of ER survey: in conventional resistance, a specified current (I) is injected into the ground using probes (current electrodes – A & B) connected to a DC power source. The resulting measured voltage (V) (across potential electrodes (M & N) is used to calculate the ground's resistance to current flow by Ohm's Law,

$$R = \frac{V}{I} \quad (4.10)$$

where R is resistance (Ohm.m), V is voltage (V), and I is current (A).

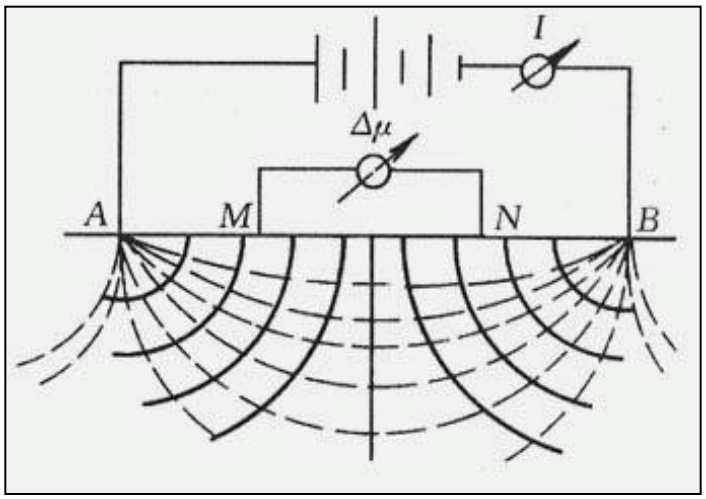

Figure 4.1 Schematic representation of electrical resistivity survey

At the landfill site, Archies's Law is the key factor that controls the resistivity of subsurface layers. Archie's equation is used to identify the electrical resistivity responses of fluid-filled porous rocks (Archie, 1942) and provide a quantitative relationship between the bulk formation resistivity (ρ_b), degree of saturation (S_n), porosity (ϕ) and pore water resistivity (ρ_w).

$$\rho_b = a\rho_w\phi^{-m}S^{-n} \quad (4.11)$$

where a (a dimensionless parameter related to the grain shape), m (a dimensionless parameter commonly referred to as the cementation exponent), and n (the saturation exponent) are material constants and empirically derived. Archie's formula is considered to be effective only for medium- to coarse-grained sediments, where the grain surface resistivity does not contribute to the bulk electrical conduction. The equation is widely used to calculate hydrocarbon saturation in ''clean'' sandstones and other relatively permeable reservoir rocks in petroleum industry. While small grain sizes dominate the lithology and/or when clay minerals are present, grain surface resistivity (ρ_s) needs to be considered and included in Archie's formula (Waxman and Smits, 1968):

$$\frac{1}{\rho_b} = \frac{\phi^m}{a\rho_w} S^n + \frac{1}{\rho_s} \text{ (4.12)}$$

The grain surface resistivity is affected by the presence of microbial cell with large surface areas, their attachment to mineral surfaces, and alteration of their host environment (Abdel Aal et al., 2004; Atekwana et al., 2004).

4.7 Magnetic susceptibility method

Magnetic susceptibility (MS) is defined as "… a measure of the ease with which a material can be magnetized" (Thompson and Oldfield, 1986). The volume magnetic susceptibility (χ_v) is defined as

$$\chi_v = M/H \text{ (4.13)}$$

where M refers to the magnetization of the material (the magnetic dipole moment per unit volume), measured in amperes per meter, H is the magnetic field strength, also measured in amperes per meter (in SI units) .There are two other measures of susceptibility: the mass magnetic susceptibility (χ_{mass}) in formula terms

$$\chi_{mass} = \kappa/\rho \text{ (4.14)}$$

where $\chi_{mass}$is the mass magnetic susceptibility in $m^3 \cdot kg^{-1}$(SI unit) or in $cm^3 \cdot g^{-1}$ in CGS, κ is the volume susceptibility and ρ is the sample bulk density ($kg \cdot m^{-3}$). And the molar magnetic susceptibility (χ_{mol}) is measured in $m^3 \cdot mol^{-1}$ (SI) or $cm^3 \cdot mol^{-1}$ (CGS), where ρ is the density in $kg \cdot m^{-3}$ (SI) or $g \cdot cm^{-3}$ (CGS) and M is molar mass in $kg \cdot mol^{-1}$ (SI) or $g \cdot mol^{-1}$ (CGS) (Dearing 1994).Since H does not change a lot along the borehole, the magnetization of material is linearly correlated with the MS, the measurement of MS can reflect the magnetization of the core sample in a landfill.

CHAPTER V

DATA ACQUISITION AND PROCESSING

5.1 Self Potential Data Acquisition and Processing

5.1.1 SP Data Acquisition

Self-potential measurements were acquired with a set of cable (1000m long, 6 Ohm.m), a high-input-impedance (50 M Ohm) voltmeter (Fluke 179 True RMS Multimeters) and two non-polarizable electrodes (made of Cu/CuSO4). The resolution of the voltmeter is 0.1 mV. Since current between the electrodes are quite small, it is essential that the impedance of the voltmeter is much larger than the impedance between electrodes in order to measure correct SP values (Corwin and Hoover, 1979). One electrode served as the base station electrode while the other served as the roving electrode. The roving electrode is used to detect the electrical potential at the ground surface to map the self-potential anomalies in this project. For each measurement, three holes with the depth of 20 cm were dug at each station so that the final SP value is an average of these three measurements. SP data were collected within 3 days in June 2012. The base station was set close to well 131 (Shown in Figure 5.1) outside the contaminated zone. A total of 60 measurements were performed over the southern part of the landfill, most of which are

located around monitoring wells. The SP measurements were acquired at locations in and outside the leachate plume area.

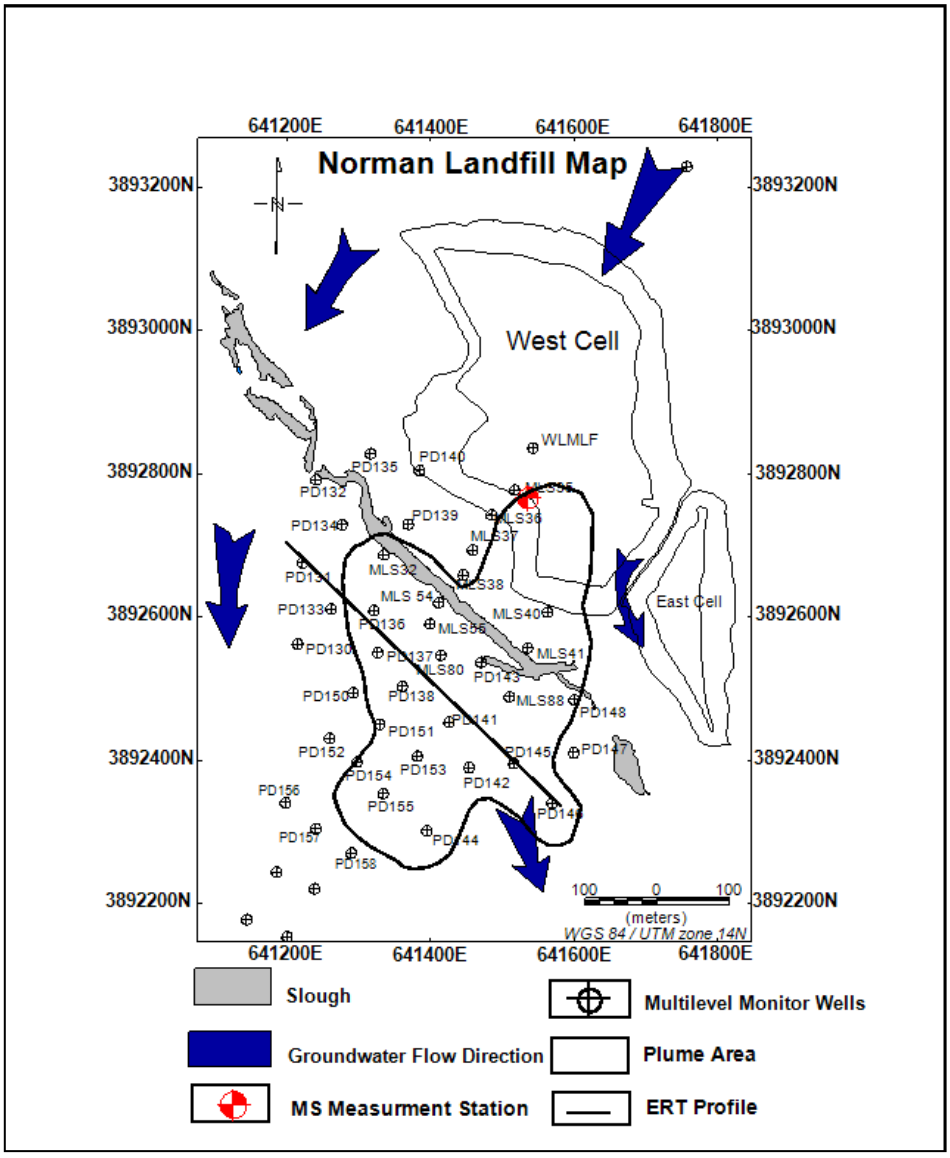

Figure 5.1Map of Geophysical Surveys. Plume outline is based on chloride concentrations Section 6.1); Magnetic suseptbility (MS) is measured next to well MLS 35 marked as red; One electrical resistivity (ER) survey profile and one SP survey profile is drawn as solid lines; most of the SP survey was conducted at monitoring well locations

5.1.2 SP Data Processing

The methods used for making SP measurements are as documented in Corry (1985) and in detail in Corry et al. (1983). The processing methods involved tie-in corrections and

drift corrections. The base tie-in corrections are defined as the absolute voltage of the base from any measurement stations within the survey area. Hence, for lines done using base station where the absolute voltage is zero, the base tie-in correction is, by definition, zero. While for other lines applying the new bases where the absolute voltage is of appropriate value, the tie-in corrections must be added to the entire line in order to refer the voltage to the survey base. However in this research tie-in corrections are not applied since the wire was long enough to reach all measurement points in the area. The drift correction in this survey involves short-time drift correction.

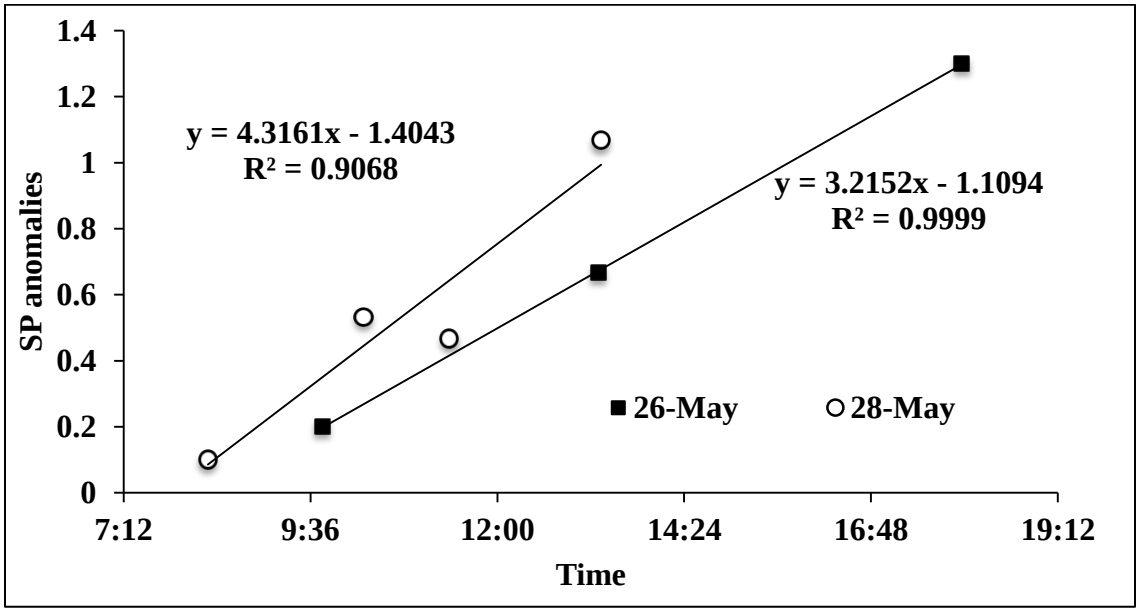

Figure 5.2 SP anomalies varying as a function of time

The differences between values measured at same points along a profile at different times were linearly interpolated or subtracted from the measurements. Based on SP results at base station in two days (Figure 5.2), data collected within 6 hours varied about +/- 1.2 mV. A linear equation describing how SP changes as a function of time can be determined. For example, the survey on May 28 2012 shows that SP increases by ~0.43 mV at the base station at 12:00, hence 0.43 mV was subtracted at the measurement

station which is recorded at 12:00 in order to reference the data to the same base station at the same time. The corrected data is included in Appendix 1

5.2 Magnetic Susceptibility (MS) Borehole Data Acquisition and Processing

MS borehole data were obtained three meters away from the well MLS 35 located within the contaminated area. The new well named "New 35" (Figure 5.1) was drilled and borehole MS data were acquired using a Barington MS probe and processed by W&R Instruments Company. The corrected MS data is included in Appendix 2.

5.3 Electrical Resistivity Data Acquisition and Processing

Electrical resistivity (ER) survey was conducted along the profile starting from well PD 146and ending near well PD 131(Figure 5.1). The profile extends from uncontaminated zones to contaminated zones and is perpendicular to the groundwater flow direction. The ER survey used a dipole-dipole array with 5 m electrode spacing. An IRIS Syscal Pro with 72 electrodes was used to acquire these data. The resistivity data were analyzed and processed by the RES2DINV software using a least-squares inversion technique (Loke and Baker, 1996).

5.4 Geochemical Data Acquisition and Processing

Most of the geochemical data used in this study were collected and analyzed by the USGS and obtained from the USGS Norman Landfill database. The multilevel wells network follow a transect parallel to the groundwater flow direction extending from the base of the landfill location to the Canadian River. The oxidation-reduction potential was measured at different levels of the wells at the Norman Landfill site using YSI 556 multi-probe meter by the author (June 2011). Groundwater elevation data were collected at all multi-level monitoring wells using water level tape by the author (June 2012) and USGS

(from 1999 to 2011). Other geochemical data used in this study were measured by USGS on June 2010: Alkalinity was measured by incremental titration (Wells and others, 1990, p. 53-56) using 0.1639 normal sulfuric acid with a 25 or 10-milliliter aliquot of a filtered sample.Field-ammonia, sulfide and ferrous iron concentrations were determined after sample collection using specific-ion and spectrophotometric techniques. Ionic strength was adjusted with a sodium-hydroxide based ionic-strength adjusting solution prior to ammonia determination by a specific ion electrode. Ferrous iron concentration was determined colorimetrically on site using the Hach AccuVac ampule phenanthroline method and a portable spectrophotometer (Hach, 1989, p. 311). Sulfide concentration was measured colorimetrically using the methylene-blue method (Hach, 1989, p. 572) and a portable spectrophotometer. Many of the sulfide determinations did not include a sample-water blank to correct for turbidity. False-positive sulfide detections may have resulted.Sulfate, chloride, fluoride, bromide, nitrite, and nitrate concentrations were measured using Waters capillary electrophoresis method number N-601. Total and dissolved organic carbon were analyzed using a Dohrmann DC-80 carbon analyzer (Schlottmann 1995).All the geochemical data were analyzed and processed by Oasis Montajsoftware using the kriging method to make contour maps. The geochemical data used in this study is included in Appendix 3

CHAPTER VI

RESULTS

6.1 Hydrogeological and Geochemical results

The ground surface at the Norman Landfill generally slopes towards the Canadian River and the elevation ranges from 332 m to 329 m. The water table elevation contour map (Figure 6.1) shows the variation in the water table elevation ranging from 330 m in the northeast to 327 m in the southwest in May 2012. The average range of changes in the groundwater during a year is about one meter (Cozzarelli et al., 2011).

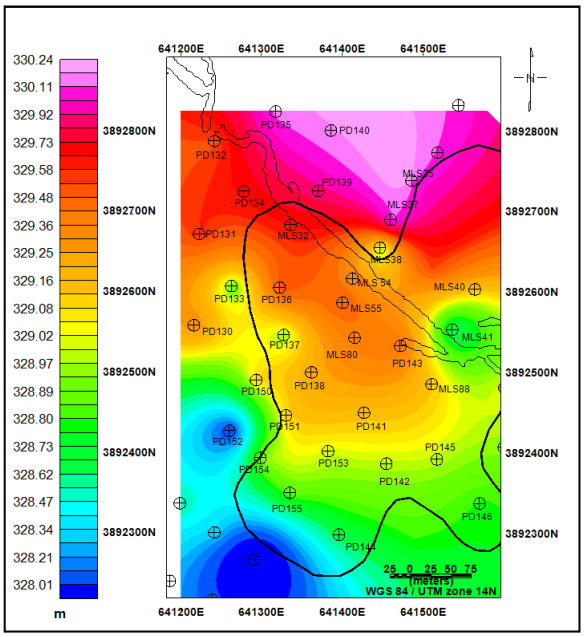

Figure 6.1 Water table elevations (Data collected by the author in 29 May, 2012).

All the geochemical data were measured at 7 depth intervals from multi-level monitor wells under groundwater from top to bottom, in this study we used the data from the

shallow zone (top level of the multi-level well, about 1 m depth), and deep zone (bottom level of the multi-level well, about 10 m depth) generated geochemical contour maps. Well PD 130, PD 131 are considered to be background wells according to the geochemistry data and previous study (e.g. Schlottmann 1995, Cozzarelli et al., 2000, Cozzarelli et al., 2011).

The shallow zone chloride distribution map (Figure 6.2.(a)) shows that chloride values range from 40 to 400 mg/L. The EPA standard for secondary maximum contaminant level for chloride is ~ 250 mg/L. High chloride concentration values (demarcated by solid black line, ranging from 200 to 400 mg/L) occur in the middle of the survey area whereas in the uncontaminated background zones (north to north-west part of the map) the concentration values are low (ranging from 10 to 200mg/L). Chloride data from deeper zones are presented in Figure 6.2 (b) and shows values ranging from 30 to 700 mg/L. High chloride concentrations (ranges from 200 to 700 mg/L) occur in the middle of the area with a strong northeasterly trend parallel to the ground water flow direction. The chloride maps suggest higher concentrations at deeper levels (denser water sinks) and that the anomaly is broader at the shallower levels but narrows at the deeper levels. The chloride data is used to delineate the leachate plume because it is common in food and other commercial products, it is negatively charged, flows "conservatively" though negatively charged aquifer and is not degraded by microbes.

The redox potential (Eh) distribution map at shallow zone is presented in Figure 6.3. Negative Eh values were observed ranging from -105 to -175 mV within the contaminated site suggesting anaerobic conditions within the plume (Cozzarelli et al., 2011). The lowest Eh values (ranging from -120 to -160 mV) occur south of the sough in

the south central part of the survey surrounded by more positive values. The most negative values occur at well site PD145. The Eh data also shows a strong east-northeasterly trend of more positive Eh values extending from the east cell of the landfill.

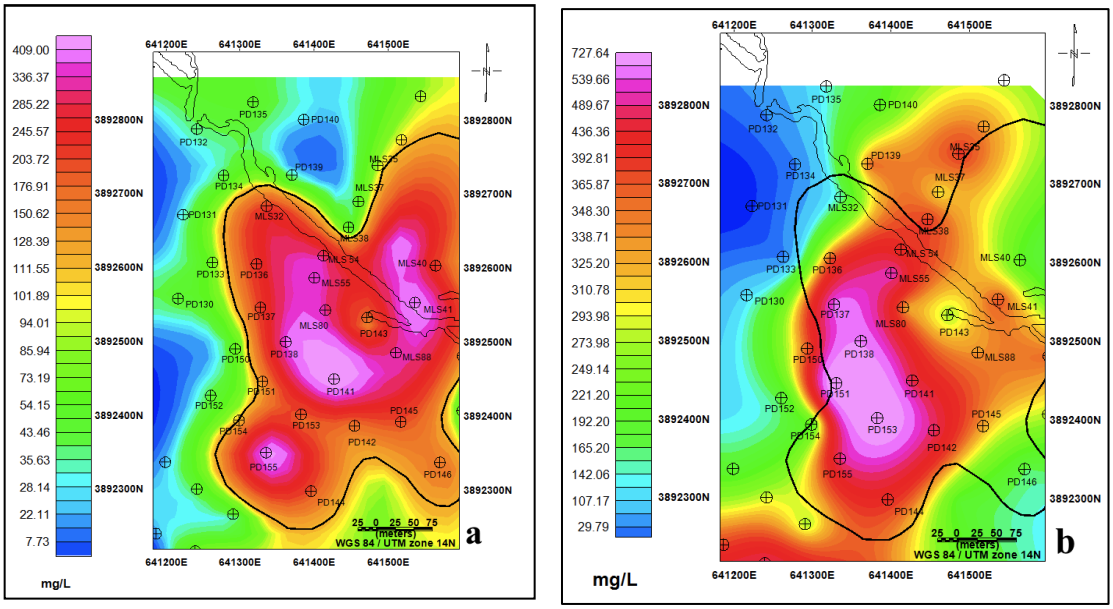

Figure 6.2 Chloride distribution map; solid line represent the plume area (Data collected by USGS in June 2010): (a) Map of shallow zone chloride distribution; (b). Map of deep zone chloride distribution.

The groundwater specific conductance values at shallow zone (Figure 6.4) range from 750 to 3400 uS/cm. As expected the specific conductance map are very similar to the chloride concentration map with a region of higher specific conductance (1500 to 3700 uS/cm) extending from the east cell of the landfill to the middle part of the survey area. The specific conductance of the leachate contaminated ground water resulted from alkalinity and chloride concentration in this area.

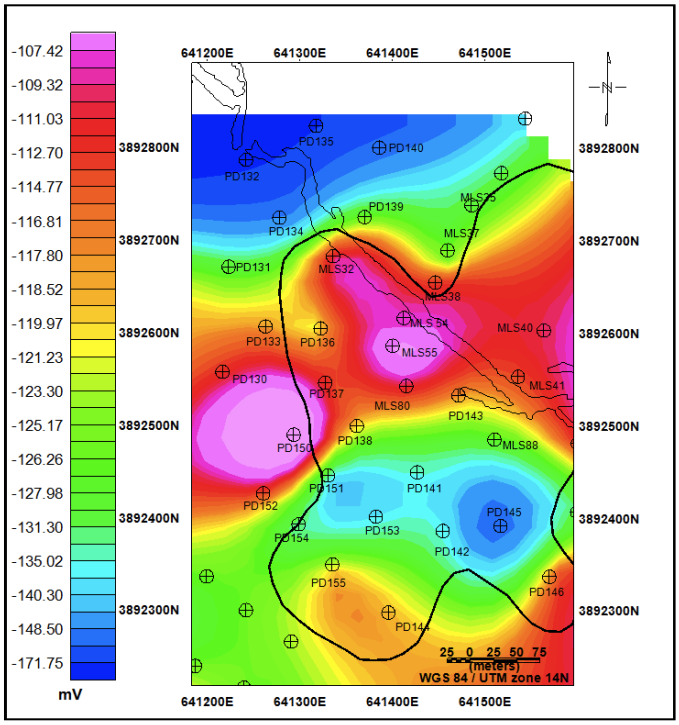

Figure 6.3Redox potential (Eh) concentration map at shallow zone (Data collected by USGS in June 2010)

Dissolved iron (Fe2+) concentration values at shallow zone (Figure 6.5) range from 1.5 to 13.5 mg/L with higher concentration >9 mg/L located in the northern part of the map and decreases from north to south. Iron concentrations were higher in water from wells downgradient of the landfill than in background well water.Dissolved iron concentrationsarehigher in the slough and downgradient of landfill than in the leachate plume area. Báez-Cazull et al. (2007) found shallow groundwater beneath the slough was greatly oversaturated with respect to siderite, and Tuttle et al. (2009) describes the abundance of FeS and pyrite in the alluvium. The high Fe2+ concentrations do not correspond toconcentrations of Cl-, HCO_3^-, or the SO_4^{2-}. This variation suggests the precipitation of secondary mineral phases or the heterogeneous availability of reactive-iron phases along the groundwater flow paths (Cozzarelli et al., 2011).Dissolved iron and

sulfate have been considered as major electron acceptors that play an important role in generating redox potentials.

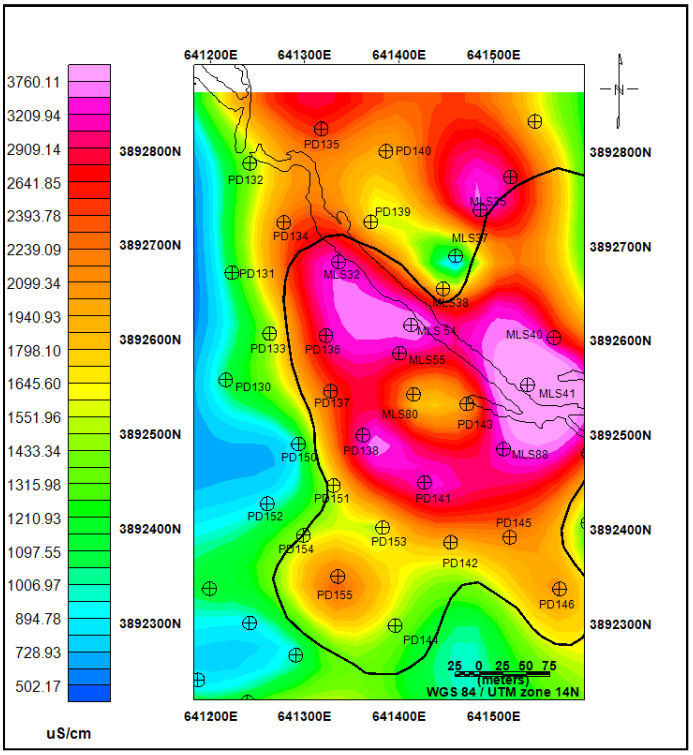

Figure 6.4 Map of groundwater conductance at shallow zone (Data collected by USGS in June 2010).

The sulfate concentration map (Figure 6.6) shows that the sulfate concentrations range from ~9 mg/L to greater than 500 mg/L at shallow zone. Except for well locations PD143 and PD136, lower sulfate values (<60 mg/L) are observed over the plume region and higher values outside the plume.Within the leachate plume area the low concentration of sulfate is due to the reduction of sulfate by microorganisms. The sulfate comes from oxidized sulfur in paper, food, wood, and other buried debris that indicates “redox” condition in this site, while dissolved iron is partially derived from waters buried in the landfill and the result from reaction of plume with sediment iron oxides (Cozzarelli et al., 2011).

Alkalinity as HCO_3^- at shallow zone is variable across the site with values ranging from 2733 mg/L within the leachate plume to values < 600 mg/L outside the plume area. Also, values are higher north of the slough> 1800mg/L compared to <1200 south of the slough (Figure 6.7). Alkalinity decreases from the landfill cell (north east) to the background area (south west) that is parallel to the groundwater flow direction. High alkalinity of the contaminated groundwater can be attributed to the degradation of organic compounds during aerobic and anaerobic oxidation of organic compounds and the presence of organic acids, the decrease of Alkalinity values away from the landfill is suggested to be the result of dilution by recharge (Schlottmann, 1995).

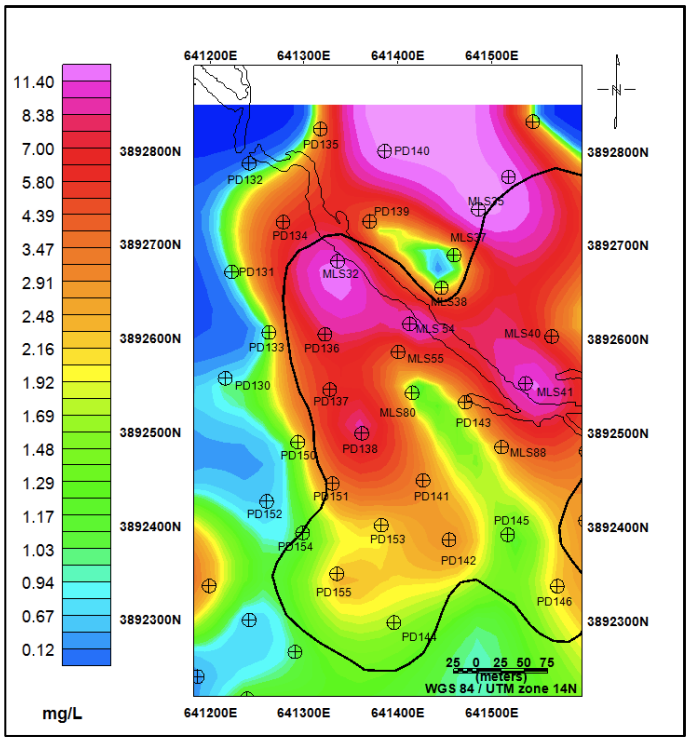

Figure 6.5 Dissolved iron concentration map at shallow zone (Data collected by USGS in June 2010.

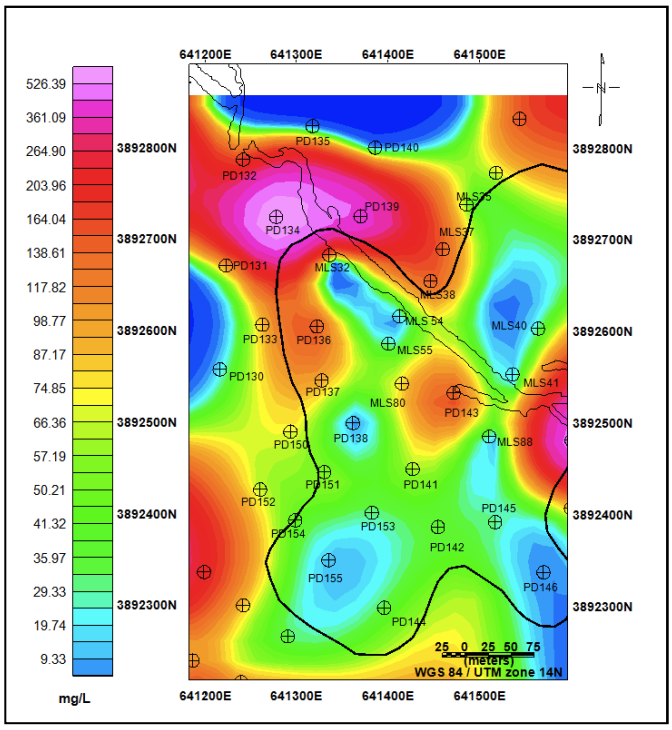

Figure 6.6 Sulfate ($SO4^{2-}$) concentration map at shallow zone.

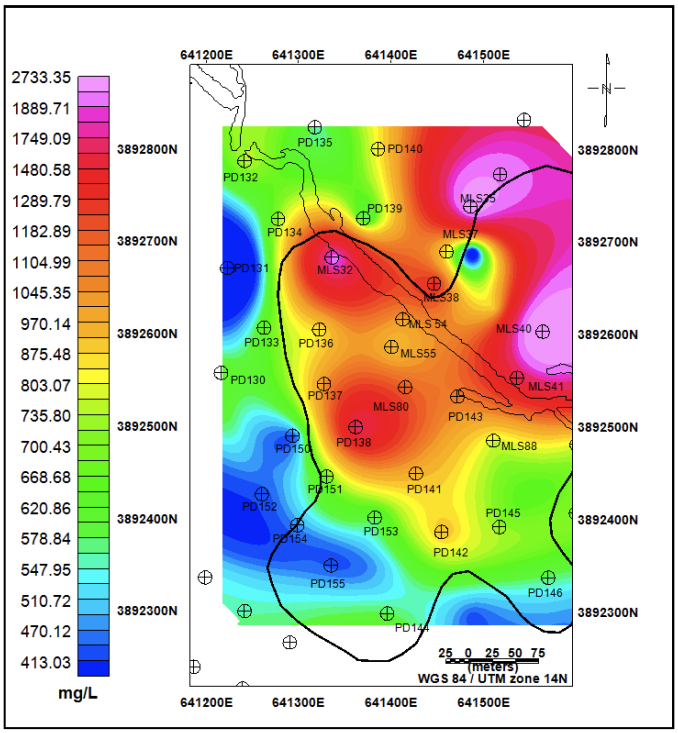

Figure 6.7 Map of alkalinity concentration at shallow zone (Data collected by USGS in June 2010).

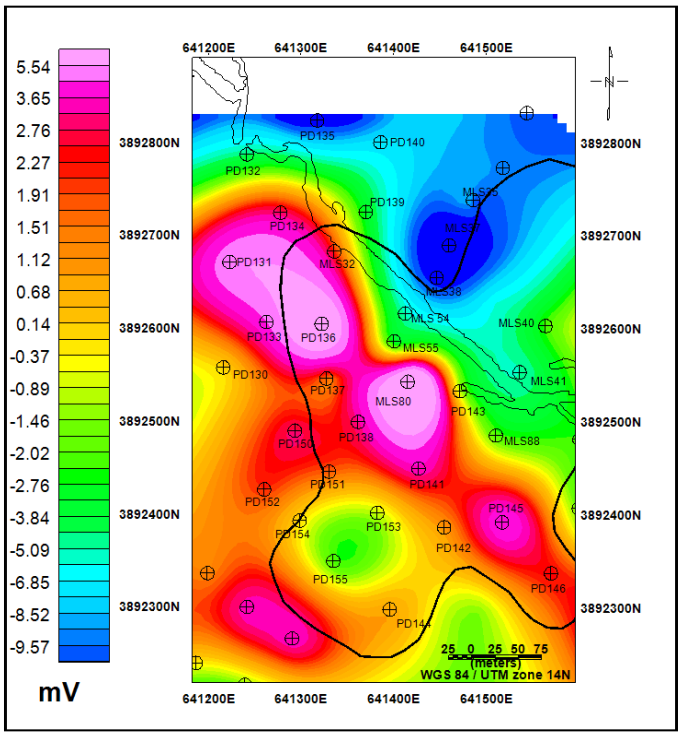

Figure 6.8 SP Contour Map (Data collected on May 2012).

6.2 Self-potential results

The SP anomaly values (Figure 6.8) range from -14 to 11 mV at this site. Negative SP values -2~-10 mV are observed north of the slough, whereas mostly positive values (0~4 mV)are found south of the slough. The most striking feature on the SP map is a NW-SE trending SP anomaly characterized by the most positive SP values observed over the site. This SP anomaly is parallel to the slough and extends from wells PD134 to PD146. Overall more positive SP values characterize the leachate plume.One SP profile (Figure5.1) was acquired over the resistivity survey line and described in section 6.1.4.

6.3 Magnetic Susceptibility (MS) borehole results

The field MS data obtained from contaminated area shows an elevated zone of MS (Figure 6.9) located from 329.46 to 329.23 m, right below the groundwater table (330.05 m, the ground surface elevation is 331.27 m) where the MS values range from 0.004 to

0.009 (SI unit) reaching a maximum at 329.35 m. Below this MS spike, the values average below 0.004 SI.WT fluctuates between 329.1 to 330 m across this well during the year indicating that this zone of high MS is within the water table fluctuating zone. To determine the magnetic minerals responsible for the elevated MS values, magnetic minerals were isolated by using a magnet bar. The 20 cm thick high MS layer is identified as greigite and goethite by X-ray Diffraction (XRD) method (Elizabeth et al., 2009) (Figure 6.10) which is caused by the action of microorganisms (Cogoini 1998; Kennedy et al., 2001). Greigite is a biomineral that forms under sulfate reducing conditions and is an iron sulfide mineral with formula Fe3S4being the sulfur equivalent of the magnetite (Fe3O4).It is formed by sulfate reducing bacteria or magnetotactic bacteria and is ferrimagnetic. Similarly to magnetite it is considered to be a half metal and therefore an electronic conductor.Coey et al. (1970) carried out conductivity measurements on synthetic greigitesamples and showed that the resistivity was in the range of 10-3~ 10-5 Ohm.m. The magnetic mineralogy in the Norman Landfill site is summarized as hematite (Fe2O3), maghemite (Fe2O3), greigite (Fe3S4) and magnetite (Fe3O4) (Cogoini, 1998).

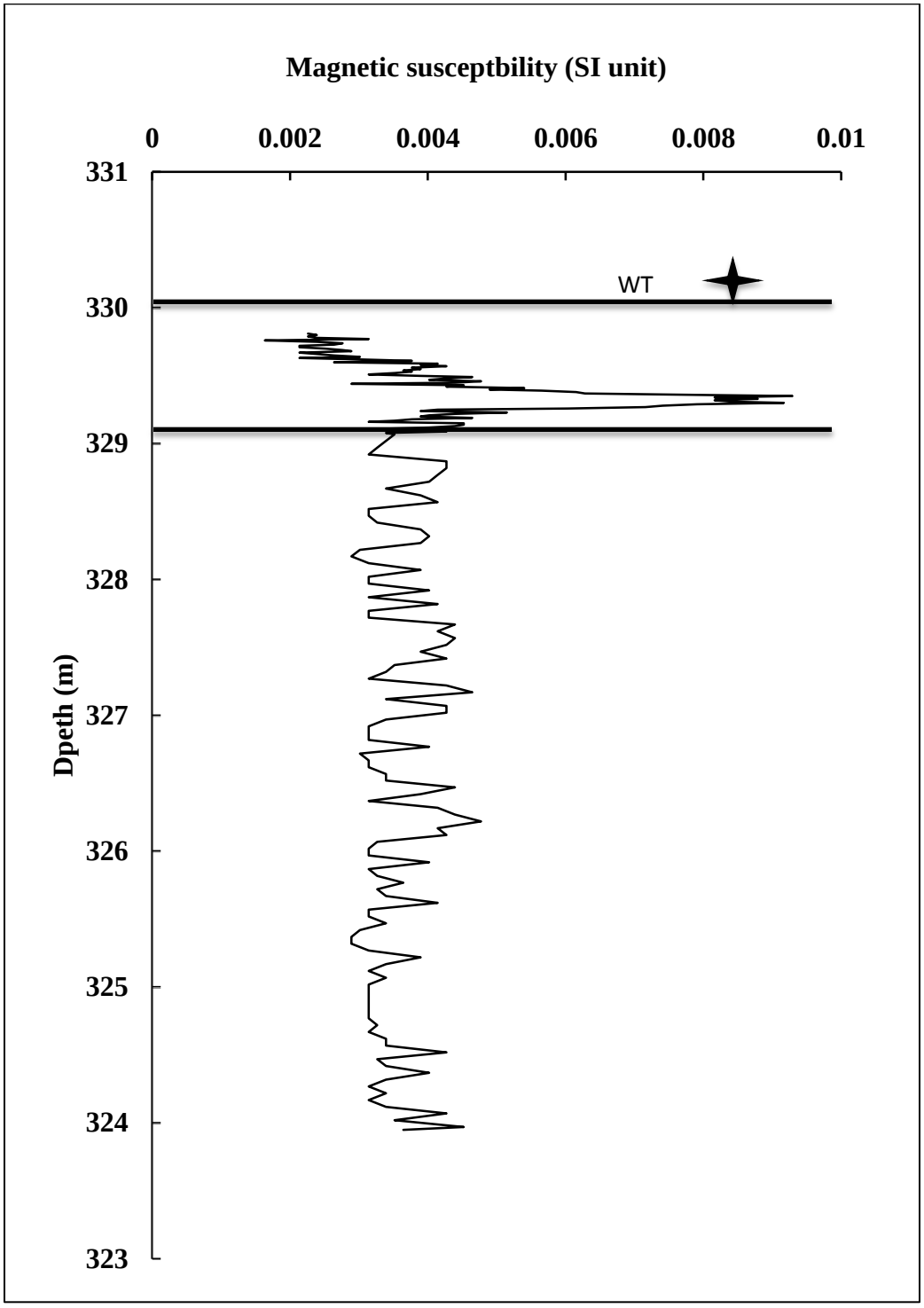

Figure 6.9 MS variations within the New35 borehole.

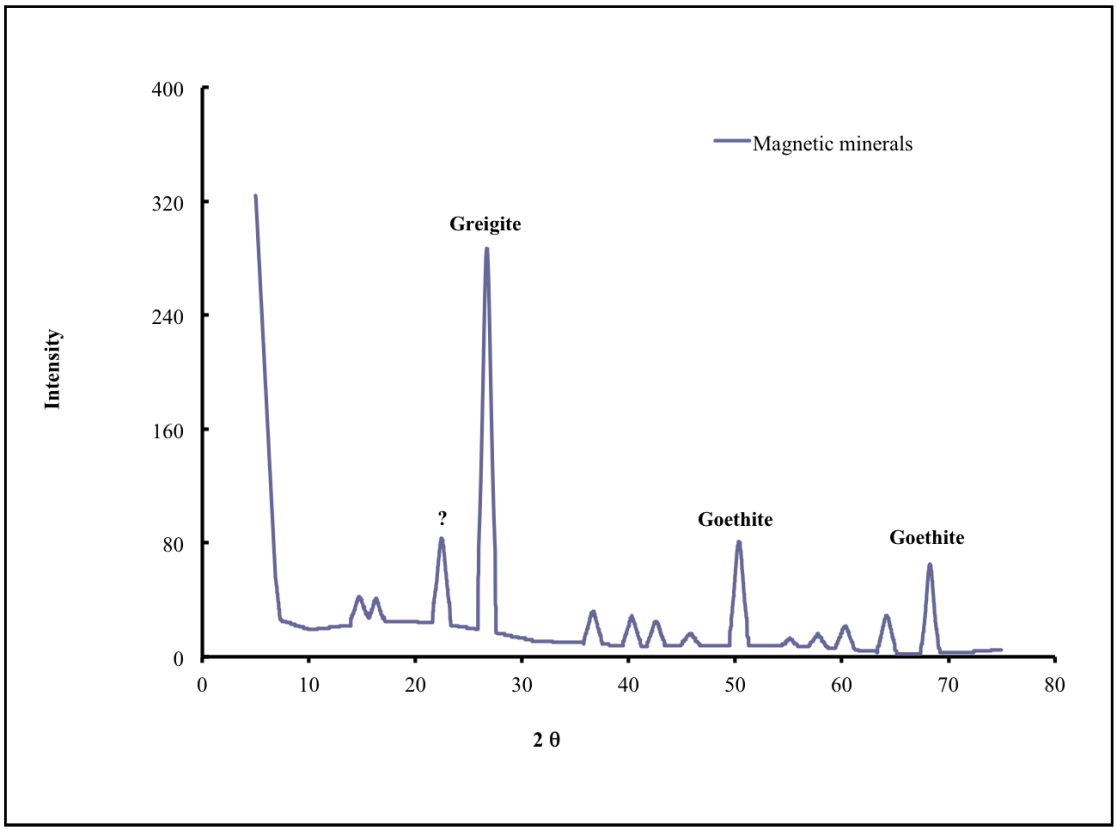

Figure 6.10 Room temperature XRD spectrum for core samples. Greigite (Fe_3S_4) and goethite is identified from the result.

6.4 Electrical resistivity results

Electrical resistivity (ER) data acquired in May 2012 were processed and the inverted resistivity profile is presented in Figure 6.11. The resistivity result shows one zone of low resistivity (<15 ohm.m) over the plume region (horizontal coordinates 200 m to 400 m) extending from near the surface into the saturated zone (vertical coordinates 8.6 m). The resistivity values in the uncontaminated regions of the vadose zone are greater than 30 Ohm.m. Zume et al. (2006) suggested that the lithology correlated with electrical conductivity at this site (Figure 6.12).

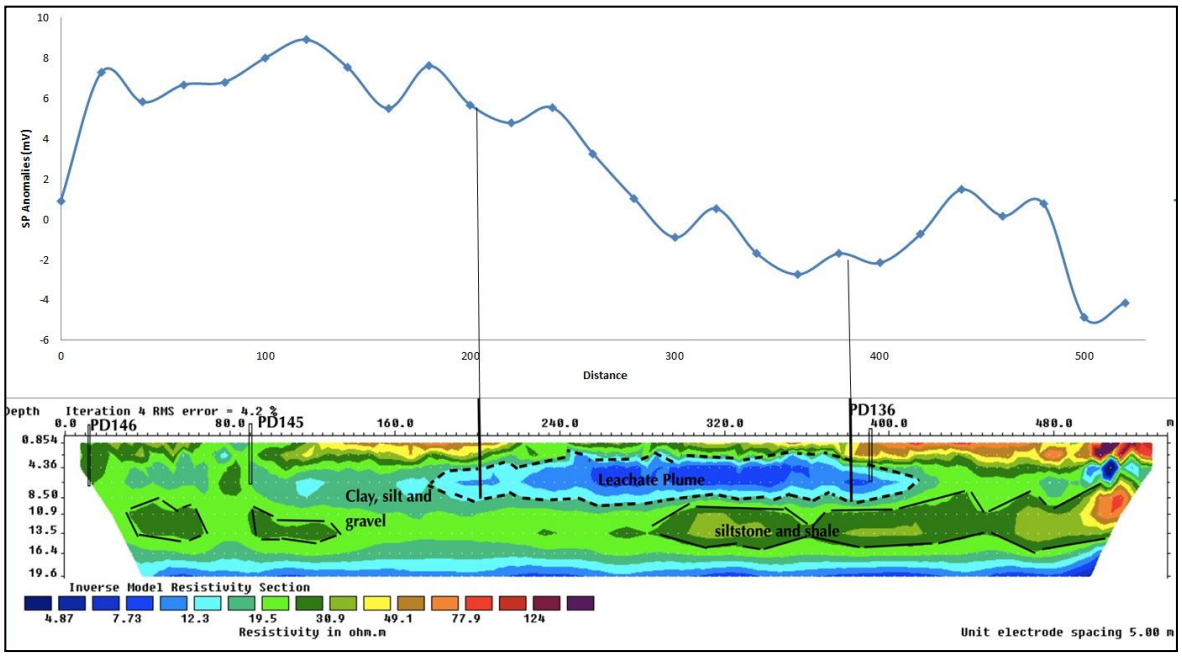

Figure 6.11 Interpreted resistivity sections and SP survey profiles at Norman Landfill Site

A high resistivity zone (yellow color, 35 to 140 ohm.m) occurs at depths <4m (horizontal coordinate 110m to 220m) where we define it as clayey sand. Below the surface there are lower resistivity zones (green color, 15~25 ohm.m) that is filled with clay, sands, pebbles and gravel. Siltstone and shale zones are characterized as higher resistivity (25~35 ohm.m) with dark green colors. Beneath that there is a bedrock layer at the depth of 16m. The relatively low resistivity compared with research done in 2006 can be attributed to the up to 4.8 cm of rain fallen 10 days prior to our survey. SP survey along the same profile was carried out and utilized to compare with ER result. Lower SP values (smaller than 6 mV) were observed coincident with the low resistivity region.However, the anomalies are not quite obvious which needs further discussion below (Chapter 7.2)

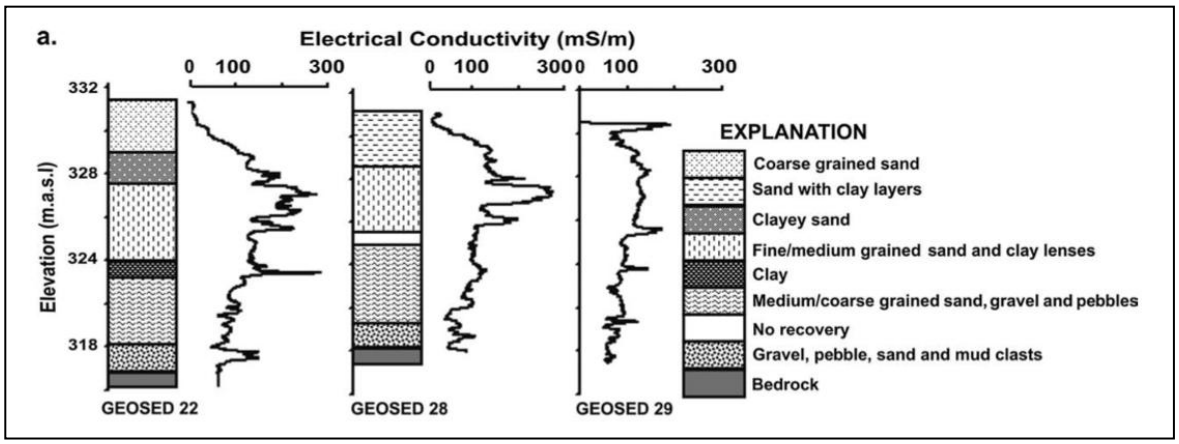

Figure 6.12Electrical conductivity logs with lithology (Zume et al., 2006)

CHAPTER VII

DISCUSSION

7.1 Variability in SP signal magnitude

The SP anomaly map (Figure 6.9) suggests that the SP anomaly values are small over the Norman landfill site ranging from ~ 8 mV to -6 mV. The small range in magnitude of SP anomalies observed over this landfill site is consistent with values observed at other organic rich contaminated sites (Sauck et al., 1998; Bavusi et al., 2006; Che-Alota et al., 2009; Forté et al., 2011) but distinctly different from those observed by Naudet et al. (2004) over the Entressen landfill in France where values in excess of ~400 mV were obtained. We also observed that the SP signals are more negative north of the slough (< -6 mV) and are more positive > -6 mV south of the slough. Also, we observe a SP positive anomaly parallel to the slough starting from well PD131 and PD134 extending to well PD146. Similar trend can be found in chloride contour map (Figure 6.2) and groundwater conductance results (Figure 6.5) showing that at shallow subsurface intervals the leachate plume extend from north west to south east which is parallel to the slough although groundwater flow is from north-east to south-west based on groundwater elevation data (Figure 5.1, Figure 6.1). Hence it is inferred that there might be two leachate plume directions: one direction coincides with the slough at shallow subsurface while the other follows the regional groundwater flow direction. Maps of geochemical parameters from samples acquired from deeper interfaces confirms this to be true (Figure 6.2 (a) and (b)).

For example, we note that the chloride concentration map shows a much broader leachate plume at the shallower depths and a more pronounced NE-SW trend in the direction of groundwater flow at the deeper levels (Figure 6.2 (b)). We note that this trend is also obvious on the water table elevation map albeit to a lesser extent. Alternatively, the strong NW-SE trend may be the result of preferential flow path or possible leachate emanating from the Asphalt plant just north of PD132.

7.2 Mechanism(s) generating the SP response over the Norman landfill plume

Several mechanisms can be used to explain the SP anomalies including streaming potential, diffusion, and biogeobattery. We evaluate the SP anomalies at the Norman landfill site in light of the above mechanisms.

7.2.1 Streaming Potential Effect

To explore a possible relationship between SP anomalies and electrochemical potentials, the electrochemical component (residual SP anomalies) have to be isolated by removing the ekectrokinetic component (streaming potentials) from the SP data. Typically the residual SP values are used to determine SP source mechanisms other than streaming potentials, however atthe Norman Landfill site it is not necessary to calculate the streaming potentials for several reasons. Naudet et al. (2004) concluded that SP anomalies are sensitive to hydraulic head difference less than 2 meters variation. However at the Norman Landfill site, the hydraulic head difference is small (most ranges only from 0 to 1 meters) suggesting that that there is not a strong effect of streaming potential. Figure 7.1 shows that the relationship between the variation of SP and water table (WT)is weak (R2=0.19). Hence the streaming potential does not significantly affect

the SP when the hydraulic head difference is so small (95% of the WT differences are less than one meter).

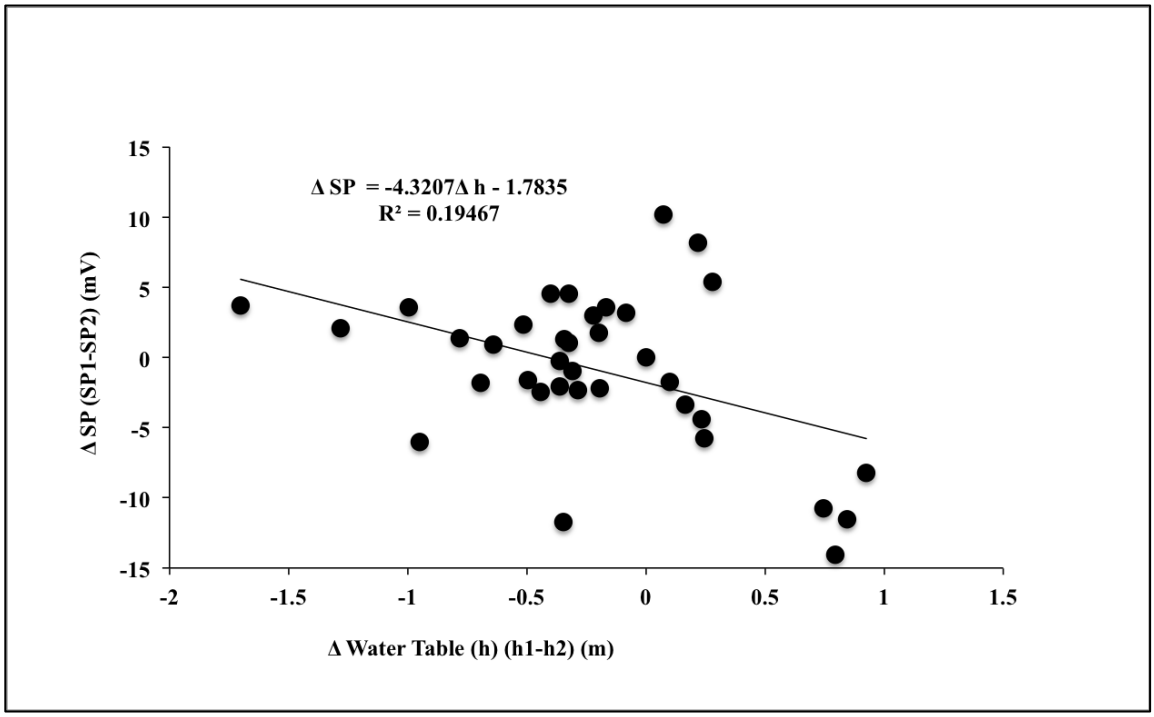

Figure 7.1SP differences vs Water table (WT) elevation differencesat Norman Landfill Site

7.2.2 Diffusion Potential Effect

Diffusion potentials, the electro-diffusion effects that arise from chemical potentials of the ionic charge carriers, were investigated as a potential mechanism that may cause the SP anomalies (Telford et al., 1990; Reynolds, 1997; Nyquist and Cory, 2002).From equation 4.8, diffusion potential contour map (Figure 7.2) within this area wascalculated based on the data frombackground well 130 and other wells within the site, large diffusion values can be attributed to the large groundwater conductance differences between background and contaminated site and the abundant species of cations and anions.

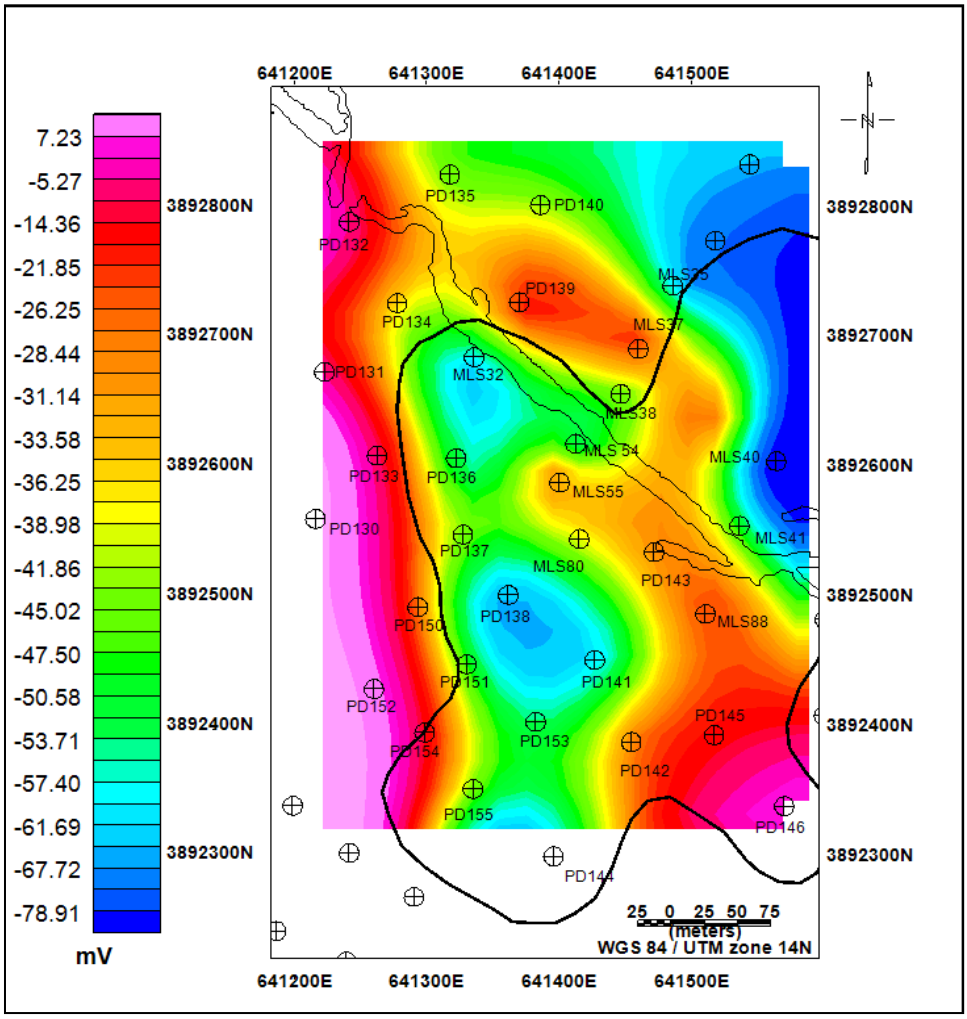

Figure 7.2Diffusion potential concentration map

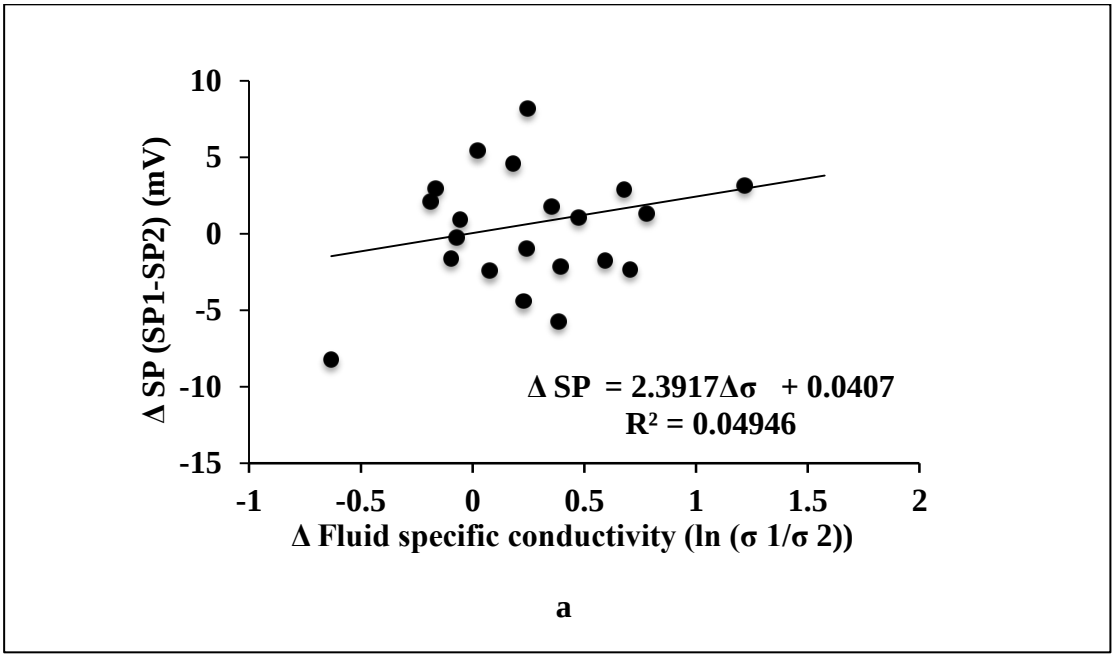

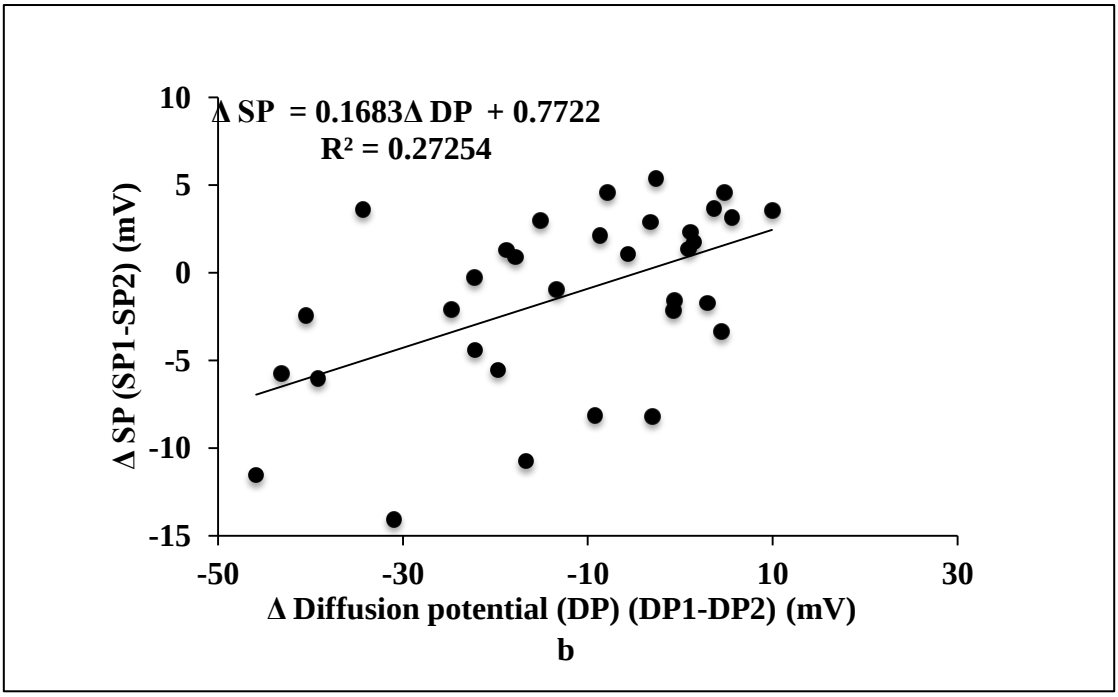

Figure 7.3Plots showing the relationship between SP and (a) Fluid conductivity, and (b) Diffusion potential

According to the diffusion contour map, we can observe the potentials range from -100 to 40 mV; negative potential signals are observed at most of the plume area ranging from -20 to -80 mV while positive potentials occur outside the contaminated area. Some studies have stated that diffusion potentials are due to differences in the mobility of electrolytes of different concentrations in pore fluids and groundwater between contaminated and background sites are the source of SP anomalies (Telford et al., 1990; Reynolds, 1997; Nyquist and Cory, 2002). Sauck et al. (1998) suggest the high SP source as being caused by electrochemical potentials from chemical concentration gradients and ion diffusion. Ionic concentration changes will affect the magnitude of diffusion potential (Equation 4.4). Removal of ions by the wet stream can reduce the ionic concentration that would potentially decrease the diffusion potentials.In order to make a more direct comparison, groundwater conductivity and diffusion values versus measured SP at well locations were plotted in Figure 7.3 (a) and 7.3 (b) separately. Although the correlation is not obvious, we can see an approximate positive linear trend between SP and diffusion potentials. Hence, diffusion potentials due to ionic concentration can be proposed as one driving source of SP.

7.2.3 Redox potential effect

At organic rich contaminated sites, TEAs processes are due to redox conditions (e.g., Figure 6.6, Figure 6.7) after the organic contaminants are degraded by microbial process (e.g., Vroblesky and Chapelle, 1994, Cozzarelli et al., 2001). At the Norman Landfill site, the dominant terminal electron-accepting processes have been identified as iron and sulfate reduction (Báez-Cazull et al., 2008). The activity of oxidized and reduced species, electron species and temperature account for important reasons of redox potential

(Equation 4.5). The spatial distribution of dissolved CO2 as bicarbonate (HCO_3^-) is an indicator of in-situ biodegradation of dissolved hydrocarbons (Van Stempvoort et al., 2002) that creates redox potentials (Figure 6.3).Naudet et al. (2003; 2004) have concluded that SP in organic rich contaminant plumes is driven by redox processes because they observed a good positive correlationbetween residual SP and redox potential (Eh). They compared the residual SP anomalies with redox potentials measured in monitoring wells and obtained a linear trend. In this survey SP is correlated with bicarbonate (Figure 7.4 (a)) and Eh (Figure 7.4 (b)) but the regression coefficient for the Norman Landfill site is poor (R2 = 0.067, R2=0.0476 respectively).

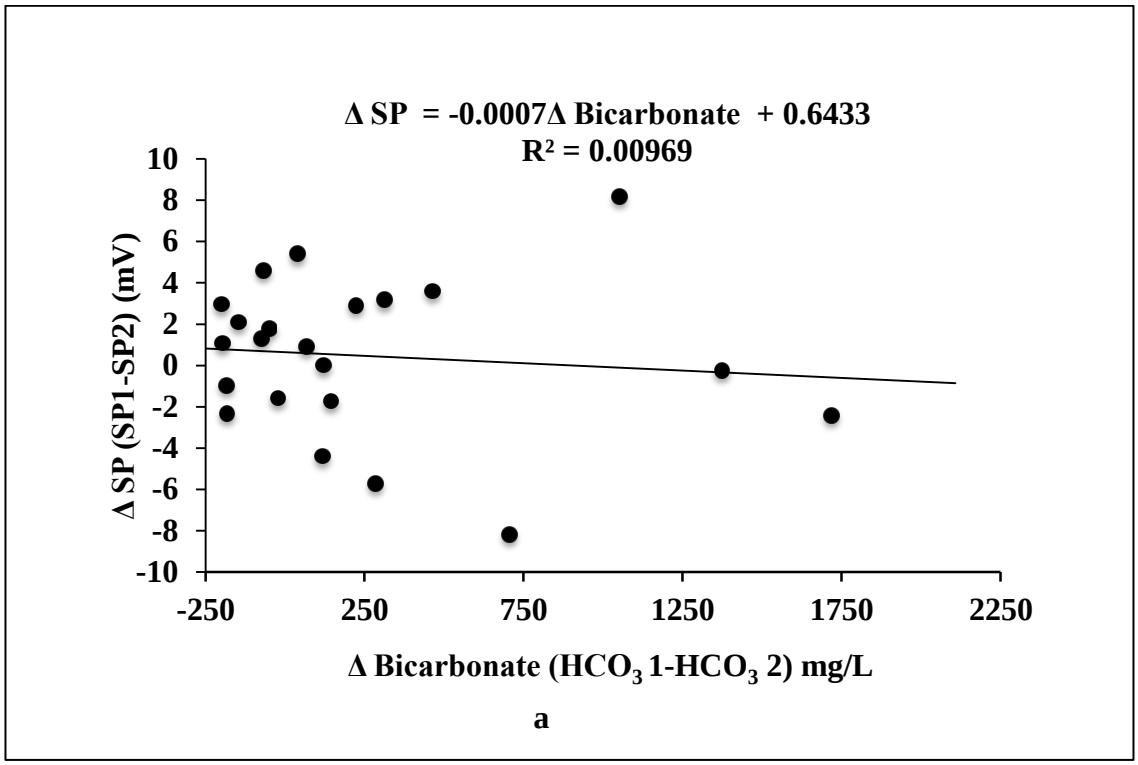

a

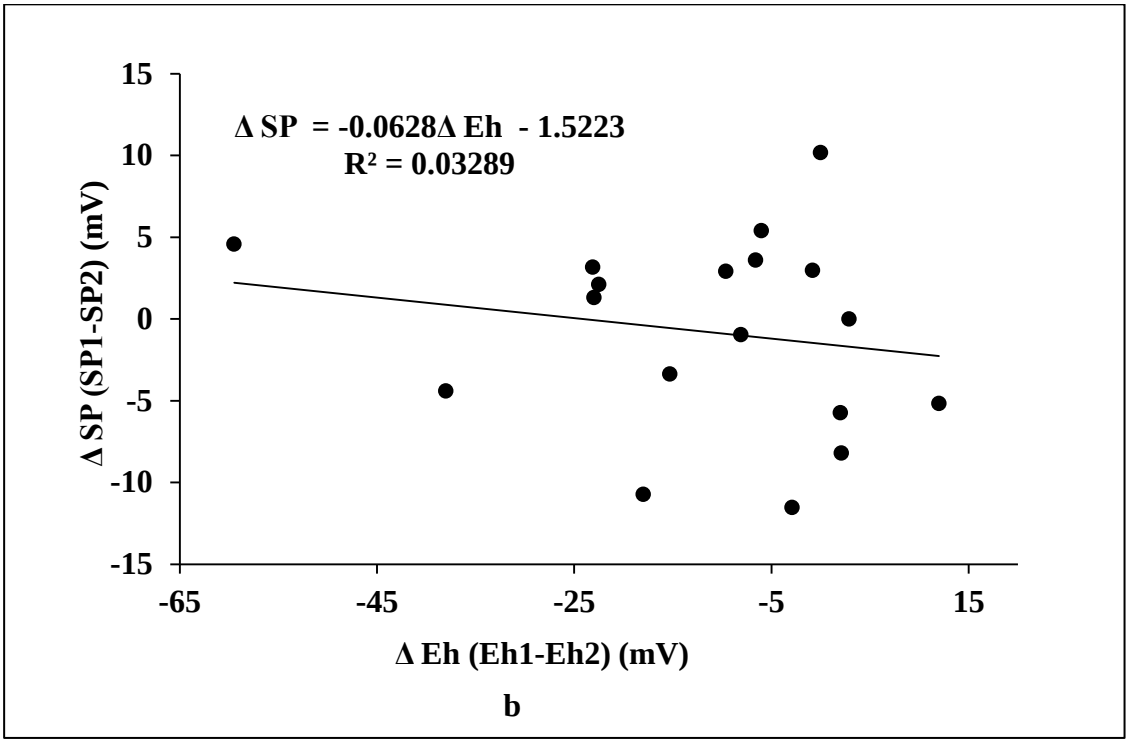

Figure 7.4Plots showing the relationship between SP and (a) bicarbonate (b). redox potential (Eh)

The reason why redox potential is not well correlated with SP can be interpreted as follows: Since Eh data were obtained from the monitoring wells below water table, the redox potentials due to biodegradation generated at capillary fringe and lower vadose zone was not detected. Hence redox measurements being compared to SP were collected from ground- water and might contribute only partly to the total SP measured at the surface (Che-Alota et al., 2009).

7.2.4 Biogeobattery model

Revil et al. (2011) proposed two biogeobattery models (Figure 1.2) in order to illustrate the SP mechanism at contaminant plume. There are two necessary conditions for the generation of large SP anomalies due to biogeobatteries: 1) large potential gradients and 2) presence of electron conductors bridging the anode and the cathode or two redox couples. According to Figure 1.2 the electronic conductors can be metallic minerals

working in concert with the microorganisms (interspecies electron transfer via conductive mineral phases; Figure 1.2 (a)) or biofilms with nanowires (Figure 1.2 (b)). The geochemistry data presented suggest active microbial degradation and negative Eh values. The MS data presented in this study suggest the existence of a high MS layer which is attributed to the presence of greigite. Greigite is a half metal and an electronic conductor similar to magnetite. A recent study by Kato et al. (2012) have clearly documented that microorganisms can use metals such as magnetite to bridge two redox couples (in their case iron reduction and nitrate reduction). Thus at the Norman landfill site, the necessary conditions for the generation of large SP anomalies exist. However, we did not observe large SP anomalies although we have the evidence of the existence of large potential gradient and the presence of electron conductors (high MS layer). We offer the following explanations for the lack of the existence of a large SP anomalies: 1). the conductive mineral phases present are disseminated and do not provide a continuous conductive path for the electron transport; 2). at the time the MS data and SP data were acquired, the high MS layer was submerged below the water table. We postulate that the position of the water table with respect to the metallic bio-mineral enriched layer plays a critical role in the generation of the large SP anomalies. In the classic Sato and Mooney geobattery model presented in Figure 1.1 a, a requirement is that the electronic conductor must straddle the water table to generate the large SP anomalies. We therefore consider the role of the water table very important in controlling biogeobatteries and we present a conceptual model to illustrate this: 1).when the metal enriched layer straddles the water table (Figure 7.5 (a)), the electronic conductors can transfer electrons from anode to cathode therefore generating a current which can result in large SP anomalies; 2) When the water table drops below the metal enriched layer (Figure 7.6(b)), the biogeobattery is

turned off and electrons cannot be transferred from electron donors to electron acceptors. As a result, no current is generated and SPanomalies are not obvious and 3)when the water table rises above the metal enriched layer (Figure 7.5(c)), the biogeobattery is turned off and electrons cannot be transferred to the cathode due to the lack of electronic conductors bridging the anode to the cathode, therefore no current flows.

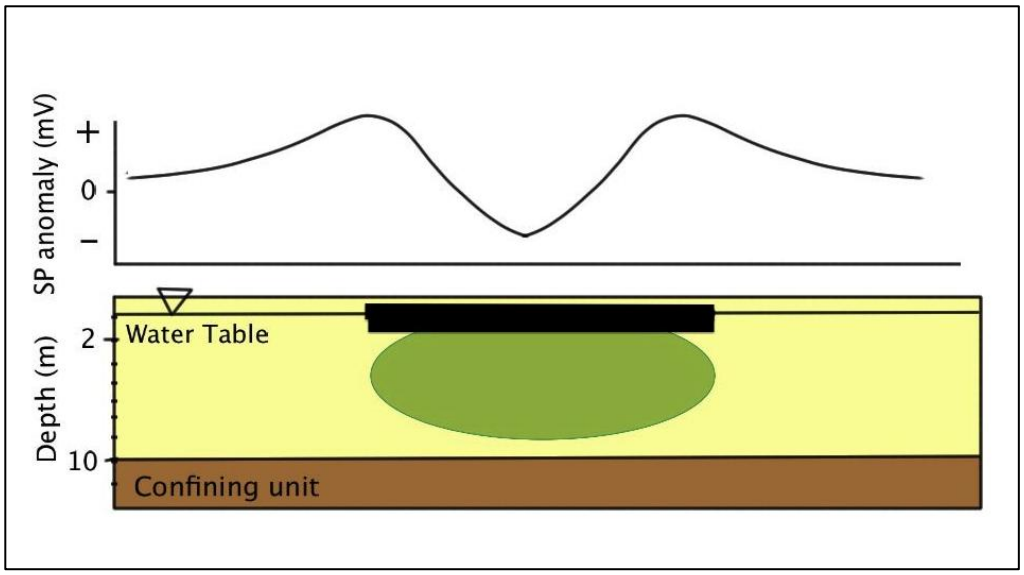

a

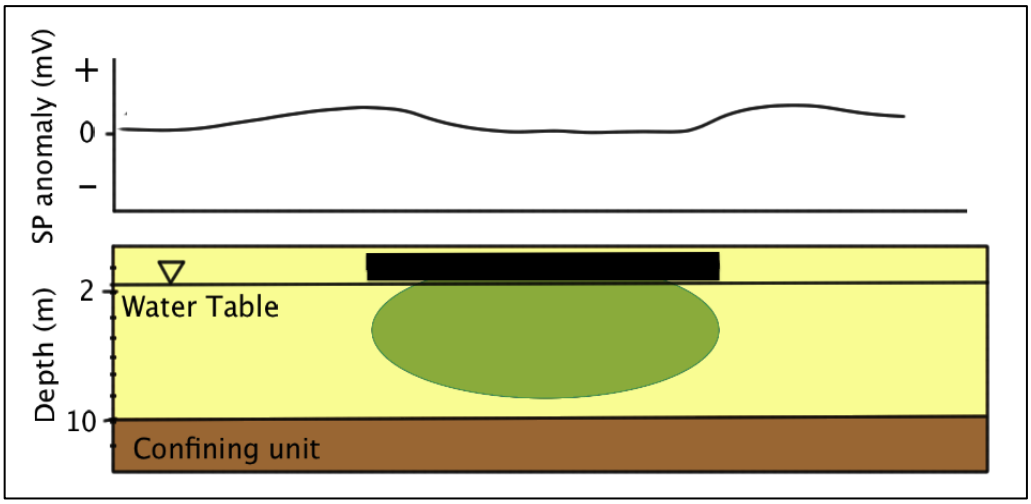

b

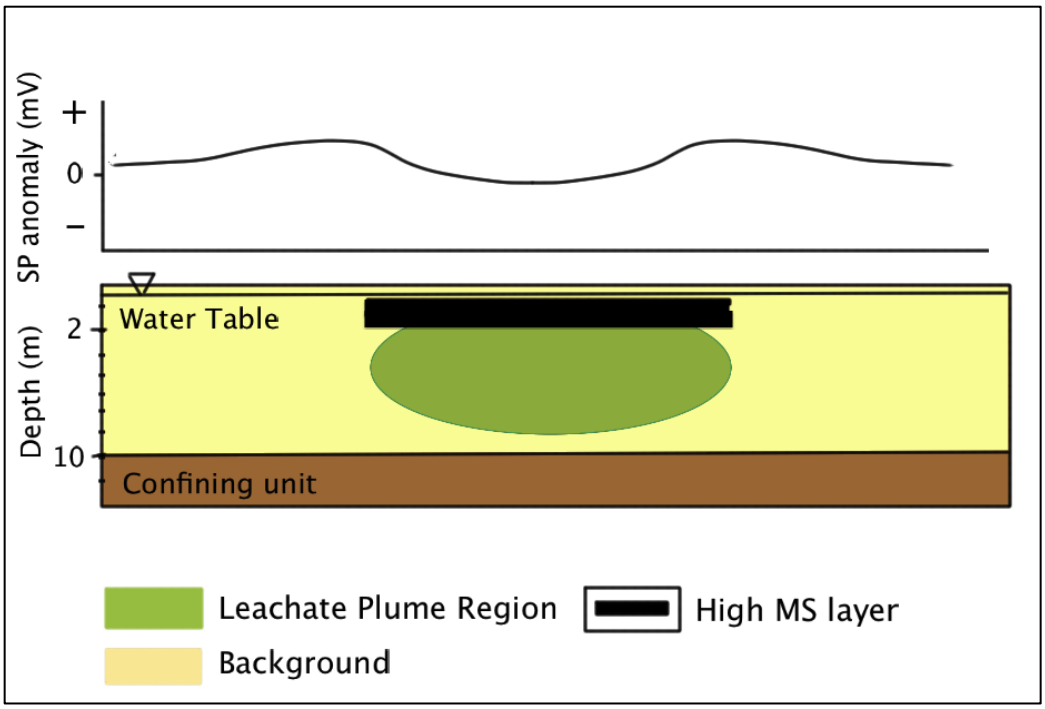

c

Figure 7.5Sketch of biogeobattery model associated with organic-rich contaminated plume.Green stands for the leachate plume region; thick black solid line stands for the high magnetic susceptibility (MS) layer. Assume groundwater flow across the section:(a). High MS layer located across the water table that can transfer the electrons from anode to cathode; (b). Water table drops therefore few electrons can be transferred from anode to cathode; (c). When water table rises above the metallic layer, electrons cannot be transferred either. Therefore water table plays an important role in generating SP signatures.

Support for the above conceptual model comes from recent studies from a hydrocarbon contaminated site in Bemidji, MN (Slater et al., unpublished data) and a study by Giampaolo et al. (2012). Slater et al. in their study (Figure 7.6) observed that downhole SP signals vary seasonally and that a transient geobattery exists at their site. SP anomalies were close to 0 mV when the electrodes were first installed (November 2010) with no variations in SP values from the surface to below the water table. However, by September 2011, the SP anomaly had increased to ~ 40 mV and showing a strong dipolar anomaly (negative above the water table and positive below the water table) as predicted by the Revil et al. (2010) shown in Figure 3.1.

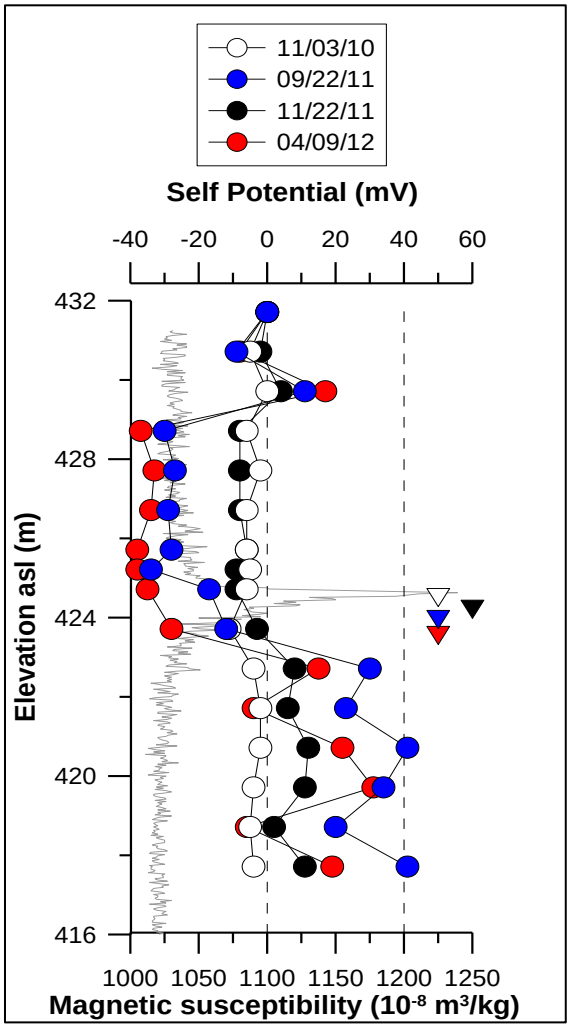

Figure 7.6 Comparison of SP signal strength as a function of water table elevation and season.

In November 2011, the anomaly decreased to 10 mV and in April 2012 increased to 30 mV. These changes in SP are tentatively related to changes in water table with respect to the magnetite layer.The data illustrates the transient nature of thegeobattery and that the SP anomaly is not always present and our ability to capture it depends on what time of the year the survey is conducted. In addition, Giampaolo et al. (2012) also documented the transient nature of the SP anomalyat a crude oil contaminated site in Trecate site (Italy). Four surface SP anomalies were conducted over the site (October 2009, March 2010, October 2010, andMarch 2011). They observed significant changesbetween SP

data acquired at different times. Mostly negative electrical potentials were observed in the October surveys whereas, positive electrical potentialswere observed in the March surveys. A further analysis of their data after removal of the streaming potential effect showed that the SP distributionwithin the contaminated zone was generally bipolar in October with the southern part of the contaminated area mostly characterized by negative values, whereas the northern part of the plume was characterized by positive values. In contrast, in March,positive SP values generally coincide with the contaminated area. The authors speculated that the water level and the height of thecapillary fringe possibly play an important role in the electrochemical mechanism. Both of these studies suggest that SP anomalies might be transient with the battery switching on and off based on changes in the concentration and gradient of redox species (related to changes in the water table elevation) that drive anodic and cathodic reactions. It is therefore conceivable that the biogeobattery model can apply to the Norman Landfill site and that the SP data presented in this study was acquired at the time when the battery was off.We therefore suggest that the source of the SP source mechanism(s) at the Norman Landfill site is diffusion potential.

CHAPTER VIII

CONCLUSIONSAND FUTURE WORK

8.1 Conclusions

Self-potential data were acquired at the surface at a landfill site in order to determine the source mechanism generating SP anomalies at organic rich contaminated sites and to test the biogeobattery model for organic rich contaminated sites. The following observations were made:

1) Small SP anomalies (ranging from 9 to -12 mV) were obtained over the landfill leachate plume;
2) SP anomaly showed poor correlation with the streaming potential and with most of the geochemical parameters measured;
3) The SP anomaly showed a weak correlation with the diffusion potential.
4) Electrical resistivity data was able to delineate the contaminated plume (ranging from 5~15 ohm.m);
5) In addition, a high magnetic susceptibility (increase from 0.004 to 0.009 SI unit) layer was found existing just below the water table interface.

Although the magnetic susceptibility data suggests the presence of metallic biominerals (greigite) capable of moving electrons across the water table interface bridging anaerobic and aerobic environments, the small SP anomalies negates the existence of a bio-

geobattery as a source of the SP anomalies at the time of the measurement. Although it is possible that the geobattery could explain the SP anomalies at the site, we speculate that it was probably turned off at the time of measurement. Instead the SP anomalies can be simply explained as resulting from diffusion potentials.

8.2 Future Work

The SP data presented in this study was acquired during one time period. Because there is evidence suggesting that SP anomalies are transient, there is a need therefore for future work that takes into consideration seasonal effects. The recommendation is as follows: 1) install borehole electrodes at several locations at the landfill site. Automate the system to make daily SP measurements including water level measurements, 2) select one profile and make surface SP measurement throughout the year including water level measurements at the time of SP measurements, 3) Surveys should also be carried out across the slough at different times of the year in order to monitor the SP variation; electrical resistivity data are needed along the same SP profile since they can define the plume precisely,4) additional borehole MS borehole data should be collected in order to confirm the existence of metallic bio-minerals that can serve aselectron conductors.

REFERENCES

Abdel Aal, G. Z., E. A. Atekwana, L. D. Slater, and E. A. Atekwana (2004), Effects of microbial processes on electrolytic and interfacial electrical properties of unconsolidated sediments, *Geophys. Res. Lett., 31*(12), L12505.

Aldana, M., V. Costanzo-Alvarez, and M. Diaz (2003), Meter Reader--Magnetic and mineralogical studies to characterize oil reservoirs in Venezuela, The Leading Edge, 22(6), 526-529.

Andrews, W. J., J. R. Masoner, and I. M. Cozzarelli (2012), Emerging Contaminants at a Closed and an Operating Landfill in Oklahoma, Ground Water Monitoring & Remediation, 32(1), 120-130.

Atekwana, E., and E. Atekwana (2010), Geophysical Signatures of Microbial Activity at Hydrocarbon Contaminated Sites: A Review, Surveys in Geophysics, 31(2), 247-283.

Atekwana, E. A., and L. D. Slater (2009), Biogeophysics: A new frontier in Earth science research, Rev. Geophys., 47(4), RG4004.

Atekwana, E. A., D. D. Werkema, and E. A. Atekwana (2006), Biogeophysics: The effects of microbial processes on geophysical properties of the shallow subsurface. Applied Hydrogeophysics, edited by H. Vereecken, A. Binley, G. Cassiani, A. Revil and K. Titov, pp. 161-193, Springer Netherlands.

Atekwana, E. A., D. D. Werkema, J. W. Duris, S. Rossbach, E. A. Atekwana, W. A.

Sauck, D. P. Cassidy, J. Means, and F. D. Legall (2004), In-situ apparent conductivity measurements and microbial population distribution at a hydrocarbon-contaminated site, Geophysics, 69(1), 56.

Atkins, P. W. (1978), Physical chemistry, W.H. Freeman, San Francisco.

Báez-Cazull, S. E., J. T. McGuire, I. M. Cozzarelli, and M. A. Voytek (2008), Determination of Dominant Biogeochemical Processes in a Contaminated Aquifer-Wetland System Using Multivariate Statistical Analysis, J. Environ. Qual., 37(1), 30-46.

Becker, C. J. (2002), Hydrogeology and leachate plume delineation at a closed municipal landfill, Norman, Oklahoma, U.S. Dept. of the Interior, U.S. Geological Survey;, Oklahoma City, OK :.

Beeman, R. E., and J. M. Suflita (1987), Microbial ecology of a shallow unconfined ground water aquifer polluted by municipal landfill leachate, Microbial Ecology, 14(1), 39-54.

Beeman, R. E., and J. M. Suflita (1990), Environmental-Factors Influencing Methanogenesis in a Shallow Anoxic Aquifer - a Field and Laboratory Study, J Ind Microbiol, 5(1), 45-58.

Bigalke, J., and E. W. Grabner (1997), The Geobattery model: a contribution to large scale electrochemistry, Electrochimica Acta, 42(23–24), 3443-3452.

Bockris, J. O. M., A. K. N. Reddy, and M. E. Gamboa-Aldeco (1998), Modern electrochemistry, Plenum Press, New York.

Breit, G. N., Program, U.S.G.S.T.S.H. and Geological, S. (2008). Results of the chemical and isotopic analyses of sediment and ground water from alluvium of the Canadian River near a closed municipal landfill, Norman, Oklahoma. Part 2,

http://purl.access.gpo.gov/GPO/LPS96546.

Buselli, G., and K. L. Lu (2001), Groundwater contamination monitoring with multichannel electrical and electromagnetic methods, J Appl Geophys, 48(1), 11-23.

Castermant, J., C. A. Mendonça, A. Revil, F. Trolard, G. Bourrié, and N. Linde (2008), Redox potential distribution inferred from self-potential measurements associated with the corrosion of a burden metallic body, Geophysical Prospecting, 56(2), 269-282.

Che-Alota, V., E. A. Atekwana, E. A. Atekwana, W. A. Sauck, and D. D. Werkema (2009), Temporal geophysical signatures from contaminant-mass remediation, Geophysics, 74(4), B113-B123.

Christenson, S. C., I. M. Cozzarelli, and S. Geological (2003), The Norman Landfill environmental research site: what happens to the waste in landfills?, edited, p. 4 p., U.S. Dept. of the Interior, U.S. Geological Survey, [Washington, D.C.].

Christenson, S. C., D. L. Parkhurst, and S. Geological (1987), Ground-water quality assessment of the central Oklahoma aquifer, Oklahoma:Project Description: U.S. Geological Survey Open-File Report 87-235, 30 p

Cogoini, M. (1997), Soil Magnetic Susceptibility Anomalies at a Landfill: Investigating Their Occurrence and Origin, University of Oklahoma.

Corry, C. E. (1985), Spontaneous Polarization Associated with Porphyry Sulfide Mineralization, Geophysics, 50(6), 1020-1034.

Corwin, R. F., and D. B. Hoover (1979), The self-potential method in geothermal exploration, Geophysics, 44(2), 226-245.

Cory, S., S. Gerondakis, and J. M. Adams (1983), Interchromosomal recombination of

the cellular oncogene c-myc with the immunoglobulin heavy chain locus in murine plasmacytomas is a reciprocal exchange, The EMBO journal, 2(5), 697-703.

Costanzo-Alvarez, V., M. Aldana, M. Diaz, G. Bayona, and C. Ayala (2006), Hydrocarbon-induced magnetic contrasts in some Venezuelan and Colombian oil wells, Earth Planets Space, 58(10), 1401-1410.

Cozzarelli, I. M., B. A. Bekins, R. P. Eganhouse, E. Warren, and H. I. Essaid (2010), In situ measurements of volatile aromatic hydrocarbon biodegradation rates in groundwater, J Contam Hydrol, 111(1-4), 48-64.

Cozzarelli, I. M., J. M. Suflita, G. A. Ulrich, S. H. Harris, M. A. Scholl, J. L. Schlottmann, and S. Christenson (2000), Geochemical and microbiological methods for evaluating anaerobic processes in an aquifer contaminated by landfill leachate, Environ Sci Technol, 34(18), 4025-4033.

Dearing, J. A. (1994), Environmental magnetic susceptibility : using the Bartington MS2 system, Chi Pub., Kenilworth.

Dearing, J. A., R. J. L. Dann, K. Hay, J. A. Lees, P. J. Loveland, B. A. Maher, and K. O'Grady (1996), Frequency-dependent susceptibility measurements of environmental materials, Geophysical Journal International, 124(1), 228-240.

Diaz, M., M. Aldana, V. Costanzo-Alvarez, P. Silva, and A. Perez (2000), EPR and magnetic susceptibility studies in well samples from some Venezuelan oil fields, Phys Chem Earth Pt A, 25(5), 447-453.

Ellwood, B. B., and B. Burkart (1996), Test of Hydrocarbon-Induced Magnetic Patterns in Soils: The Sanitary Landfill as Laboratory, Memoirs-American Association of Petroleum Geologists (66), 91-98.

Fitterman, D. V. (1979), Calculations of self-potential anomalies near vertical contacts, Geophysics, 44(2), 195-205.

Fitterman, D. V. (1979), Theory of Electrokinetic-Magnetic Anomalies in a Faulted Half-Space, J. Geophys. Res., 84(B11), 6031-6040.

Forté, S. (2011), Mapping organic contaminant plumes in groundwater using spontaneous potentials, Ph.D. thesis, University of Calgary (Canada), Canada.

Furlong, E. T., S. Geological, and L. National Water-Quality (2008), Determination of human-health pharmaceuticals in filtered water by chemically modified styrene-divinylbenzene resin-based solid-phase extraction and high-performance liquid chromatography/mass spectrometry, edited, U.S. Dept. of the Interior, U.S. Geological Survey, Reston, Va.

Gautam, P. B., U. Gautam,E. Appel (2005), Magnetic susceptibility of dust-loaded leaves as a proxy of traffic-related heavy metal pollution in Kathmandu city, Nepal, Atmospheric Environment, 39(2201－2211).

Giampaolo, V. R., E.K. Titov,A. Maineult,V. Lapenna (2012), Self-potential monitoring of a crude oil contaminated site (Trecate, Italy): first results of the modeling. 2012, EGU General Assembly Conference, 14, 5842

Gorby, Y. A., et al. (2006), Electrically conductive bacterial nanowires produced by Shewanella oneidensis strain MR-1 and other microorganisms, P Natl Acad Sci USA, 103(30), 11358-11363.

Halsall, C. J., B. A. Maher, V. V. Karloukovski, P. Shah, and S. J. Watkins (2008), A novel approach to investigating indoor/outdoor pollution links: Combined magnetic and PAH measurements, Atmospheric Environment, 42(39), 8902-8909.

Hammann.M, R.H. Maurer, G. A. Green, and H. Horstmeyer (1997), Self-Potential Image Reconstruction: Capabilities and Limitations, Journal of Environmental and Engineering Geophysics, 2(1), 21-35.

Hanesch, M. H., and R. S. Scholger (2002), Mapping of heavy metal loadings in soils by means of magnetic susceptibility measurements, Environmental Geology, 42(8), 857-870.

Hay, K. L., J. A. Dearing, S. M. J. Baban, and P. Loveland (1997), A preliminary attempt to identify atmospherically-derived pollution particles in English topsoils from magnetic susceptibility measurements, Physics and Chemistry of The Earth, 22(1-2), 207-210.

Hoffmann, V., M. Knab, and E. Appel (1999), Magnetic susceptibility mapping of roadside pollution, Journal of Geochemical Exploration, 66(1-2), 313-326.

Hubbard, C. G., L. J. West., K. Morris., B. Kulessa., D. Brookshaw., J. R. Lloyd., and S. Shaw (2011), In search of experimental evidence for the biogeobattery, Geophysical Research.

Ishido, T., and J. W. Pritchett (1999), Numerical simulation of electrokinetic potentials associated with subsurface fluid flow, J Geophys Res-Sol Ea, 104(B7), 15247-15259.

Kapièka, A., E. Petrovský, and N. Jordanova (1997), Comparison of in-situ Field Measurements of Soil Magnetic Susceptibility with Laboratory Data, Studia Geophysica et Geodaetica, 41(4), 391-395.

Kato, S., K. Hashimoto, and K. Watanabe (2012), Microbial interspecies electron transfer via electric currents through conductive minerals. Proc. Natl Acad. Sci. USA 109, 10042–10046

Keller, G. V., and F. C. Frischknecht (1966), Electrical methods in geophysical prospecting, Pergamon Press.

Kennedy, L. G., and J. W. Everett (2001), Microbial degradation of simulated landfill leachate: solid iron/sulfur interactions, Advances in Environmental Research, 5(2), 103-116.

Linde, N., D. Jougnot, A. Revil, S. K. Matthai, T. Arora, D. Renard, and C. Doussan (2007), Streaming current generation in two-phase flow conditions, Geophys Res Lett, 34(3).

Liu, Q., Q. Liu, L. Chan, T. Yang, X. Xia, and T. Cheng (2006), Magnetic enhancement caused by hydrocarbon migration in the Mawangmiao Oil Field, Jianghan Basin, China, Journal of Petroleum Science and Engineering, 53(1-2), 25-33.

Loke, M. H., and R. D. Barker (1996), Rapid least-squares inversion of apparent resistivity pseudosections by a quasi-Newton method1, Geophysical Prospecting, 44(1), 131-152.

Lovley, D. R. (2008), Extracellular electron transfer: wires, capacitors, iron lungs, and more, Geobiology, 6(3), 225-231.

Maher, B. A., and R. Thompson (1999), Quaternary Climates, Environments and Magnetism, Cambridge University Press.

Maineult, A., L. Jouniaux, and Y. Bernabe (2006), Influence of the mineralogical composition on the self-potential response to advection of KCl concentration fronts through sand, Geophys Res Lett, 33(24).

Martins, C. C., M. M. Mahiques, M. C. Bicego, M. M. Fukumoto, and R. C. Montone (2007), Comparison between anthropogenic hydrocarbons and magnetic susceptibility in sediment cores from the Santos Estuary, Brazil, Mar Pollut Bull,

54(2), 240-246.

Mendonca, C. A. (2008), Forward and inverse self-potential modeling in mineral exploration, Geophysics, 73(1), F33-F43.

Mewafy, F. M., E. A. Atekwana, D. D. Werkema, Jr., L. D. Slater, D. Ntarlagiannis, A. Revil, M. Skold, and G. N. Delin (2011), Magnetic susceptibility as a proxy for investigating microbially mediated iron reduction, Geophys. Res. Lett., 38(21), L21402.

Minsley, B. J., J. Sogade, and F. D. Morgan (2007), Three-dimensional self-potential inversion for subsurface DNAPL contaminant detection at the Savannah River Site, South Carolina, Water Resour. Res., 43(4), W04429.

Mooney, H. M. (1960), The Electrochemical Mechanism of Sulfide Self-Potentials - Reply, Geophysics, 51(1), 196-196.

Morris, A.W, K.J. Versteeg, H.C. Marvin, E.B. Mccarry, and A.N. Rukavina (1994), Preliminary comparisons between magnetic susceptibility and polycyclic aromatic hydrocarbon content in sediments from Hamilton Harbour, western Lake Ontario, 152(2).

Naudet, V., and A. Revil (2005), A sandbox experiment to investigate bacteria-mediated redox processes on self-potential signals, Geophys. Res. Lett., 32(11), L11405.

Naudet, V., A. Revil, J. Y. Bottero, and P. Begassat (2003), Relationship between self-potential (SP) signals and redox conditions in contaminated groundwater, Geophys Res Lett, 30(21).

Naudet, V., A. Revil, E. Rizzo, J. Y. Bottero, and P. Begassat (2004), Groundwater redox conditions and conductivity in a contaminant plume from geoelectrical investigations, Hydrol Earth Syst Sc, 8(1), 8-22.

Nielsen, L. P., N. Risgaard-Petersen, H. Fossing, P. B. Christensen, and M. Sayama (2010), Electric currents couple spatially separated biogeochemical processes in marine sediment, 463\(7284\), 1071\-1074\.

Ntarlagiannis, D., E. A. Atekwana, E. A. Hill, and Y. Gorby (2007), Microbial nanowires: Is the subsurface "hardwired"?, Geophysics. Res. Lett., 34(17), L17305.

Nyquist, J. E., and C. E. Corry (2002), Self-potential: The ugly duckling of environmental geophysics, The Leading Edge, 21(5), 446-451.

Petrovský, E, Ellwood, B. B, Maher, A. Barbara, and Thompson, Roy (1999), Magnetic monitoring of air- land- and water-pollution. Quaternary Climates, Environments and Magnetism, Cambridge University Press.

Pirson, S. J. (1981), Quantification of magento-electrotelluric exploration results, Bull. South Tex. Geol. Soc., 21:7, 23-30.

Reguera, G., K. D. McCarthy, T. Mehta, J. S. Nicoll, M. T. Tuominen, and D. R. Lovley (2005), Extracellular electron transfer via microbial nanowires, Nature, 435(7045), 1098-1101.

Revil, A., and P. Leroy (2001), Hydroelectric coupling in a Clayey Material, Geophys Res Lett, 28(8), 1643-1646.

Revil, A., C. A. Mendonca, E. A. Atekwana, B. Kulessa, S. S. Hubbard, and K. J. Bohlen (2010), Understanding biogeobatteries: Where geophysics meets microbiology, J Geophys Res-Biogeo, 115.

Revil, A., V. Naudet, J. Nouzaret, and M. Pessel (2003), Principles of electrography applied to self-potential electrokinetic sources and hydrogeological applications, Water Resour Res, 39(5).

Revil, A., F. Trolard, G. Bourrie, J. Castermant, A. Jardani, and C. A. Mendonca (2009), Ionic contribution to the self-potential signals associated with a redox front, J Contam Hydrol, 109(1-4), 27-39.

Reynolds, J. M. (2011), An Introduction to Applied and Environmental Geophysics, edited, John Wiley & Sons, Hoboken.

Risgaard-Petersen. N., A. Revil,P. Meister, and P. L. Nielsen (2012), Sulfur, iron-, and calcium cycling associated with natural electric currents running through marine sediment. Geochim. Cosmochim. Acta 92, 1–13.

Rijal, M. L., E. Appel, E. Petrovský, and U. Blaha (2010), Change of magnetic properties due to fluctuations of hydrocarbon contaminated groundwater in unconsolidated sediments, Environmental Pollution, 158(5), 1756-1762.

Rizzo, E., B. Suski, A. Revil, S. Straface, and S. Troisi (2004), Self-potential signals associated with pumping tests experiments, J. Geophys. Res., 109(B10), B10203.

Christenson, C. S., and I.M. Cozzarelli (1999), Geochemical and microbiological processes in ground water and surface water affected by municipal landfill leachate, U.S. Geological Survey Toxic Substances Hydrology Program, Proceedings of the Technical Meeting, Charleston, 3(SC March 8-12), 499-500.

Sauck, W. A., E. A. Atekwana, and M. S. Nash (1998), High Conductivities Associated with an LNAPL Plume Imaged By Integrated Geophysical Techniques, Journal of Environmental and Engineering Geophysics, 2(3), 203-212.

Schlottmann, J. L., and S. Geological (2001), Water chemistry near the closed Norman Landfill, Cleveland County, Oklahoma, 1995, v, 44 p. pp., U.S. Dept. of the Interior, U.S. Geological Survey ; Branch of Information Services [distributor], Oklahoma City, OK : Denver, CO.

Spiteri, C., V. Kalinski, W. Rösler, V. Hoffmann, E. Appel, and M. team (2005), Magnetic screening of a pollution hotspot in the Lausitz area, Eastern Germany: correlation analysis between magnetic proxies and heavy metal contamination in soils, Environmental Geology, 49(1), 1-9.

Stoll, J., J. Bigalke, and E. W. Grabner (1995), Electrochemical modelling of self-potential anomalies, Surveys in Geophysics, 16(1), 107-120.

Strzyszcz, Z., T. Magiera, and F. Heller (1996), The influence of industrial immissions on the magnetic susceptibility of soils in upper Silesia, Studia Geophysica et Geodaetica, 40(3), 276-286.

Suski, B., A. Revil, K. Titov, P. Konosavsky, M. Voltz, C. Dages, and O. Huttel (2006), Monitoring of an infiltration experiment using the self-potential method, Water Resource Res, 42(8).

Tarling, D. H. (1983), Palaeomagnetism, New York ;, London; Chapman and Hall.

Telford, W. M., L. P. Geldart, and R. E. Sheriff (1990), Applied Geophysics, Cambridge University Press.

Thompson, K. F., J. Holt, and G. Kennedy (1997), Eh Mapping Locates Petroleum Seepage: Using electrical potential to "high-grade" seafloor sediments for natural seepage and potential reserves, Sea Technology, 38(7), 47-53.

Thompson, R., and F. Oldfield (1986), Environmental magnetism, Allen & Unwin, London; Boston.

Timm, F., and P. Möller (2001), The relation between electric and redox potential: evidence from laboratory and field measurements, Journal of Geochemical Exploration, 72(2), 115-128.

Tuttle, M. L. W., G. N. Breit, and I. M. Cozzarelli (2009), Processes affecting ä34S and

ä18O values of dissolved sulfate in alluvium along the Canadian River, central Oklahoma, USA, Chemical Geology, 265(3–4), 455-467.

Vichabian, Y., and F. D. Morgan (1999), Self Potential Monitoring of Jet Fuel Air Sparging, Symposium on the Application of Geophysics to Engineering and Environmental Problems, 12(1), 549-553.

Vroblesky, D. A., and F. H. Chapelle (1994), Temporal and spatial changes of terminal electron-accepting processes in a petroleum hydrocarbon-contaminated aquifer and the significance for contaminant biodegradation, Water Resour. Res., 30(5), 1561-1570.

Waxman, M. H., and L. J. M. Smits (1968), Electrical Conductivities in Oil-Bearing Shaly Sands, SPEJ Society of Petroleum Engineers Journal, 8(2).

Weigel, M. (1989), Self-potential surveys on waste dumps theory and practice, Detection of Subsurface Flow Phenomena, edited by G.-P. Merkler, H. Militzer, H. Hötzl, H. Armbruster and J. Brauns, pp. 109-120, Springer Berlin / Heidelberg.

Werkema, D. D. (2003), Investigating the geoelectrical response of hydrocarbon contamination undergoing biodegradation, Geophys. Res. Lett. Geophysical Research Letters, 30(12).

Williams, K. H., S. S. Hubbard, and J. F. Banfield (2007), Galvanic interpretation of self-potential signals associated with microbial sulfate-reduction, J. Geophys. Res., 112(G3), G03019.

Wood, P. R., and L. C. Burton (1968), Ground-water resources in Cleveland and Oklahoma Counties, Oklahoma, University of Oklahoma, Norman.

Zaugg, S. D., S. G. Smith, M. P. Schroeder, S. Geological, and L. National Water-

Quality (2006), Determination of wastewater compounds in whole water by continuous liquid-liquid extraction and capillary-column gas chromatography/mass spectrometry, edited, U.S. Dept. of the Interior, U.S. Geological Survey, Reston, Va.

Zume, J. T., A. Tarhule, and S. Christenson (2006), Subsurface Imaging of an Abandoned Solid Waste Landfill Site in Norman, Oklahoma, Ground Water Monitoring & Remediation, 26(2), 62-6

APPENDICE

Appendix 1

Table 1 Well identification, well location, Self potential, Redox potential (Eh), water table elevation, Fluid specific conductance, Fe^{2+}, HCO_3^-, Cl^-, SO_4^{2-} in groundwater from shallow zone of multilevel monitoringwells

Well ID	X_UTM14	Y_UTM14	*SP (mV)	*Eh (mV)	Water table elevation (m)	Specific Conductance (us/cm)	Dissolved Iron Fe^{2+} (mg/L)	Bicarbonate (HCO_3^-) (mg/L)	Chloride (Cl^-) (mg/L)	Sulfate (SO_4^{2-}) (mg/L)
Background Location										
PD130	641217.07	3892561.52	0.00	-112.00	329.02	1155	1.07	627.45	50.72	26.06
PD131	641223.83	3892674.97	5.40		329.23	1182	1.04	701.00	33.45	80.45
PD132	641242.60	3892790.75	-4.40	-109.10	329.40	1452	0.47	748.16	40.08	150.21
PD134	641278.71	3892728.08	2.90	-150.00	329.30	2276	5.33	745.00	36.65	715.85
PD135	641318.48	3892827.26	-11.53	-171.50	330.02	1179	4.43	559.85	19.98	157.48
PD136	641323.30	3892608.33	8.17	-121.60	329.13	1477	6.36	850.51	21.11	108.50
Plume Fringe										
PD133	641263.68	3892610.40	4.57	-118.00	329.92	1385	1.03	667.23	72.01	89.39
PD139	641370.90	3892728.73			330.14	1575	1.25	553.39	8.91	484.30
PD152	641261.21	3892430.30	2.10	-112.80	328.80	957	0.68	428.65	50.03	57.84
MLS36	641486.40	3892692.60	-8.20		329.96	614	0.59	277.78	9.16	95.62
Plume Core										
PD137	641328.37	3892549.56	1.30	-114.90	329.01	2519	5.98	1069.64	330.00	3.28
PD138	641362.58	3892502.90	3.17		328.91	3901	9.45	1678.58	372.27	3.87
PD141	641427.85	3892452.70	3.60	-135.00	328.82	1896	2.46	940.01	167.29	60.88

PD142	641455.53	3892389.35	1.07	-135.10	328.72	1857	2.98	920.09	148.26	36.81
PD143	641472.61	3892535.98	-1.73	-118.60	329.02	2093	5.12	1091.96	128.97	52.92
PD144	641485.89	3892298.63	-1.60		328.57	1050	0.97	430.53	77.44	72.21
PD148	641601.67	3892484.07	-2.33		328.87	2339	3.14	772.18	125.46	520.36
PD149	641391.50	3892290.50	0.90		328.57	1094	1.02	606.00	78.44	103.40
PD150	641294.25	3892493.50	2.97		328.89	979	1.77	444.78	49.07	76.54
PD151	641331.11	3892449.45	1.77		328.86	1646	3.39	695.00	123.49	66.51
PD153	641383.30	3892404.93	-0.97		328.77	1470	1.98	577.85	160.66	30.02
PD154	641299.51	3892396.79	-0.27	-134.50	328.70	1077	1.34	481.14	66.58	41.58
PD155	641335.90	3892353.22	-2.43	-120.10	328.60	1249	3.51	442.97	73.21	153.94
MLS32	641336.81	3892686.36			329.25	3410	12.82	2001.00	251.37	1.75
MLS35	641486.75	3892741.50	-10.73		329.92	3595	16.72	2345.00	95.77	42.56
MLS37	641460.72	3892692.71	-14.07	-130.00	329.78	1617	1.01	784.37	34.76	147.11
MLS38	641447.40	3892657.94	-11.73	-109.90	328.57	2651	4.10	1333.92	185.32	34.94
MLS40	641564.92	3892606.05			329.19	5581	8.37	2734.73	319.93	119.40
MLS43	641509.53	3892632.32	-5.73		329.23	1698	0.04	892.27	29.86	167.87
MLS54	641413.35	3892619.54			329.19	1813	2.92	1010.59	84.83	21.17
MLS55	641401.26	3892589.59	10.17	-100.00	329.14	1666	0.46	912.38	75.38	47.61
MLS88	641511.42	3892488.24	-2.17	-127.30	328.91	1712	1.02	767.34	90.77	160.49

*Eh data were collected by the author on July 2011; SP data were collected by the author on May 2012.
The missing data of Eh is caused by the low water table during dry season (July 2011); Missing SP data is because the author cannot reach the well location due to the thick vegetation.

Appendix 2

Table 2. Borehole Magnetic Susceptibility data for well "New 35"

Elevation (m)	Magnetic Susceptibility (SI Unit)
329.81	0.0022608
329.8	0.0023864
329.79	0.0022608
329.78	0.0023864
329.77	0.00314
329.76	0.0016328
329.75	0.0023864
329.74	0.0027632
329.73	0.0026376
329.72	0.0021352
329.71	0.0021352
329.7	0.002512
329.69	0.0027632
329.68	0.0028888
329.67	0.0021352
329.66	0.0023864
329.65	0.0026376
329.64	0.0030144
329.63	0.0021352
329.62	0.0030144
329.61	0.003768
329.6	0.0026376
329.59	0.0041448
329.58	0.0038936
329.57	0.0042704
329.56	0.003768
329.55	0.0038936
329.54	0.0036424
329.53	0.003768
329.52	0.0035168
329.51	0.00314
329.5	0.0038936
329.49	0.0046472
329.48	0.0042704

329.47	0.0040192
329.46	0.0047728
329.45	0.004396
329.44	0.0028888
329.43	0.0045216
329.42	0.0042704
329.41	0.0054008
329.4	0.0048984
329.39	0.005652
329.38	0.0061544
329.37	0.00628
329.36	0.0079128
329.35	0.0092944
329.34	0.008164
329.33	0.008792
329.32	0.008164
329.31	0.0084152
329.3	0.0091688
329.29	0.0079128
329.28	0.0074104
329.27	0.0071592
329.26	0.0060288
329.25	0.0041448
329.24	0.0038936
329.23	0.0051496
329.22	0.004396
329.21	0.0040192
329.2	0.0038936
329.19	0.0046472
329.18	0.003768
329.17	0.0035168
329.16	0.00314
329.15	0.0045216
329.14	0.0045216
329.13	0.004396
329.12	0.0040192
329.11	0.0033912
329.1	0.0032656
329.09	0.0042704
329.08	0.0033912

329.07	0.0035168
329.02	0.0033912
328.97	0.0032656
328.92	0.00314
328.87	0.0042704
328.82	0.0042704
328.77	0.0041448
328.72	0.0040192
328.67	0.0033912
328.62	0.0038936
328.57	0.0041448
328.52	0.00314
328.47	0.00314
328.42	0.0032656
328.37	0.0038936
328.32	0.0040192
328.27	0.0038936
328.22	0.0030144
328.17	0.0028888
328.12	0.00314
328.07	0.0038936
328.02	0.00314
327.97	0.00314
327.92	0.0040192
327.87	0.00314
327.82	0.0041448
327.77	0.00314
327.72	0.00314
327.67	0.004396
327.62	0.0041448
327.57	0.004396
327.52	0.0042704
327.47	0.0038936
327.42	0.0042704
327.37	0.0035168
327.32	0.0033912
327.27	0.00314
327.22	0.0042704
327.17	0.0046472
327.12	0.0033912

327.07	0.0042704
327.02	0.0042704
326.97	0.0033912
326.92	0.00314
326.87	0.00314
326.82	0.00314
326.77	0.0040192
326.72	0.0030144
326.67	0.00314
326.62	0.00314
326.57	0.0033912
326.52	0.0033912
326.47	0.004396
326.42	0.0038936
326.37	0.00314
326.32	0.0041448
326.27	0.004396
326.22	0.0047728
326.17	0.0041448
326.12	0.0042704
326.07	0.0032656
326.02	0.00314
325.97	0.00314
325.92	0.0040192
325.87	0.00314
325.82	0.0032656
325.77	0.0036424
325.72	0.0032656
325.67	0.0033912
325.62	0.0041448
325.57	0.00314
325.52	0.00314
325.47	0.0033912
325.42	0.0030144
325.37	0.0028888
325.32	0.0028888
325.27	0.00314
325.22	0.0038936
325.17	0.0033912
325.12	0.00314

325.07	0.0033912
325.02	0.00314
324.97	0.00314
324.92	0.00314
324.87	0.00314
324.82	0.00314
324.77	0.00314
324.72	0.0032656
324.67	0.00314
324.62	0.0033912
324.57	0.0033912
324.52	0.0042704
324.47	0.0032656
324.42	0.0033912
324.37	0.0040192
324.32	0.0033912
324.27	0.00314
324.22	0.0033912
324.17	0.00314
324.12	0.0033912
324.07	0.0042704
324.02	0.0035168
323.97	0.0045216
323.95	0.0036424

Appendix 3

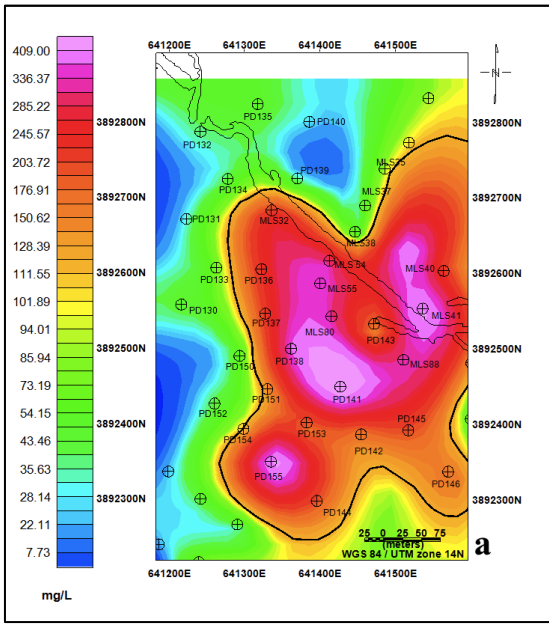

Figure 1.a Chloride distribution map at shallow depth

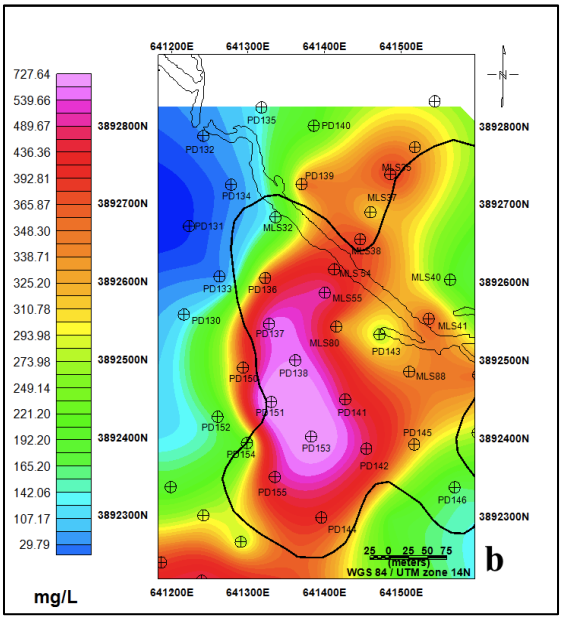

Figure 1.b Chloride distribution map at deep depth

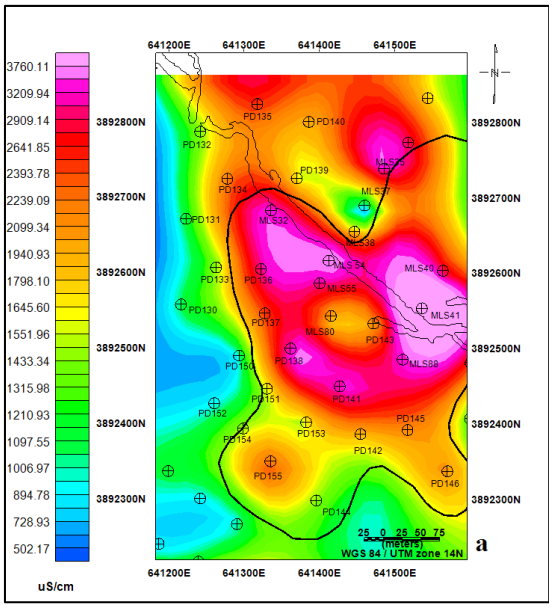

Figure 2.aFluid specific conductance distribution map at shallow depth

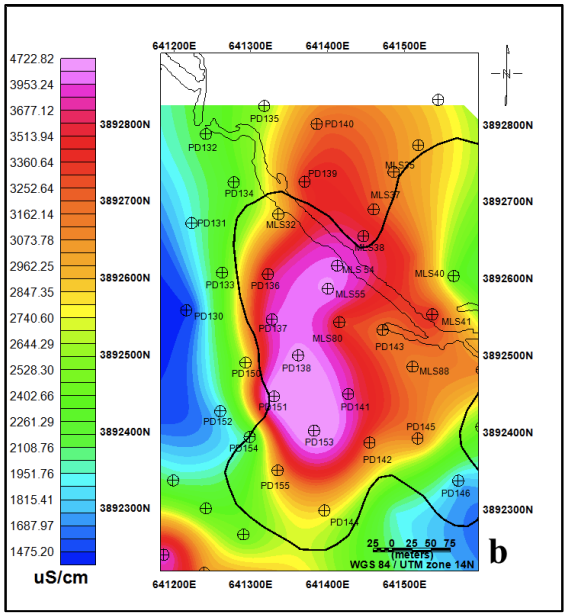

Figure 2.b Fluid specific conductance distribution map at deep depth

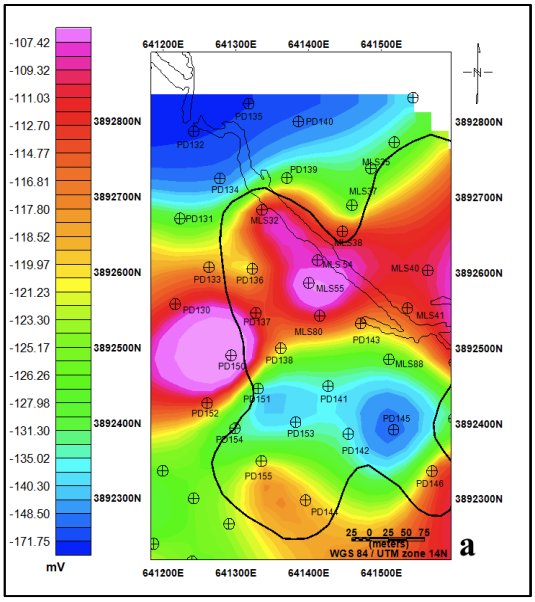

Figure 3.a Redox Potential (Eh) concentration map at shallow depth

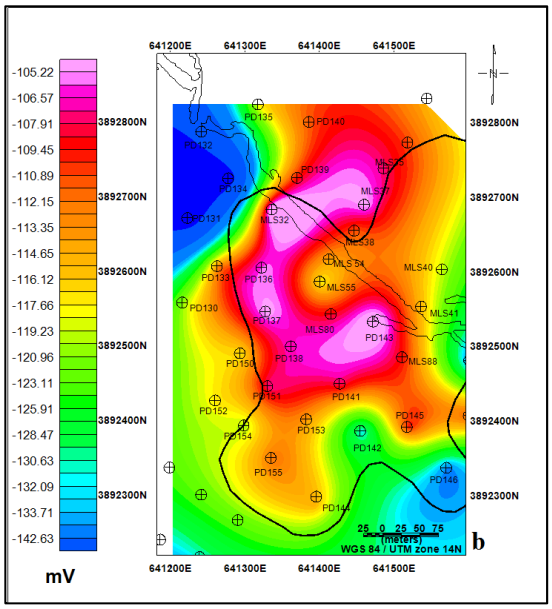

Figure 3.b Redox Potential (Eh) concentration map at deep depth

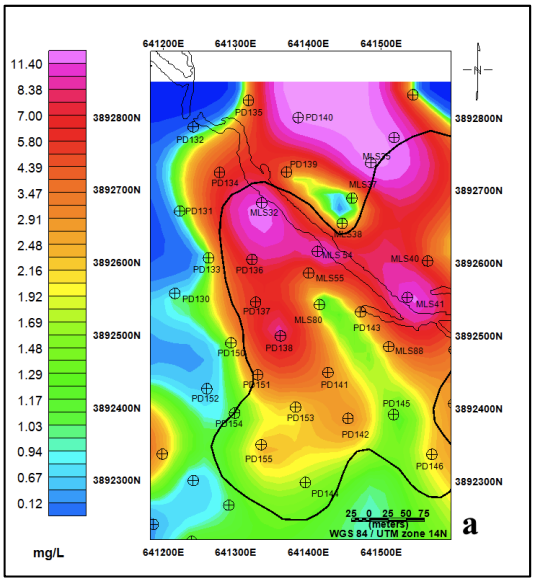

Figure 4.a Dissolved iron distribution map at shallow depth

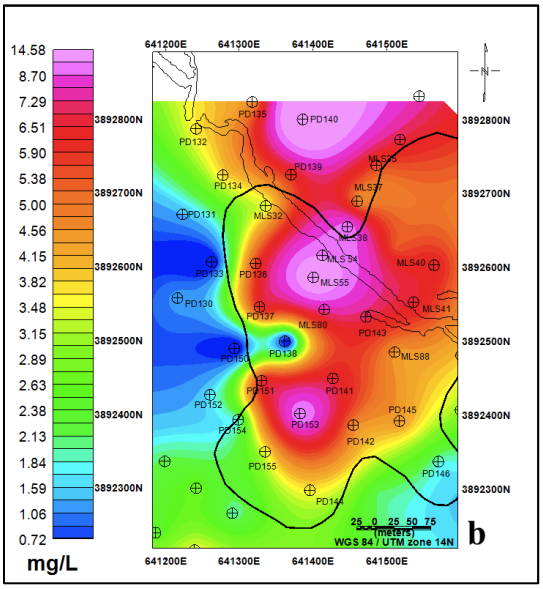

Figure 4.b Dissolved iron distribution map at deep depth

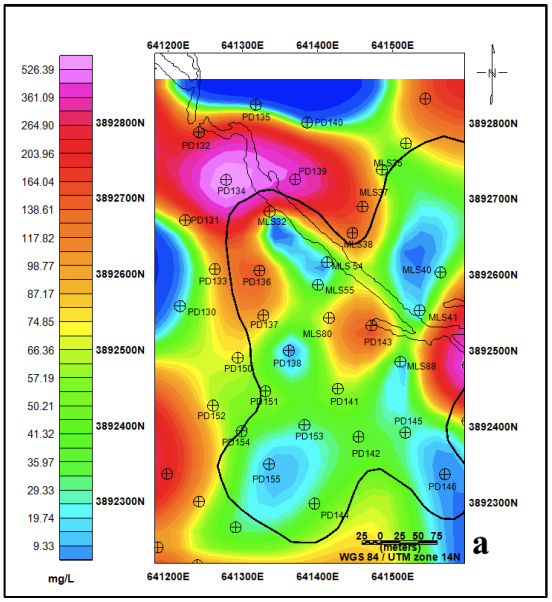

Figure 5.a Sulfate distribution map at shallow depth

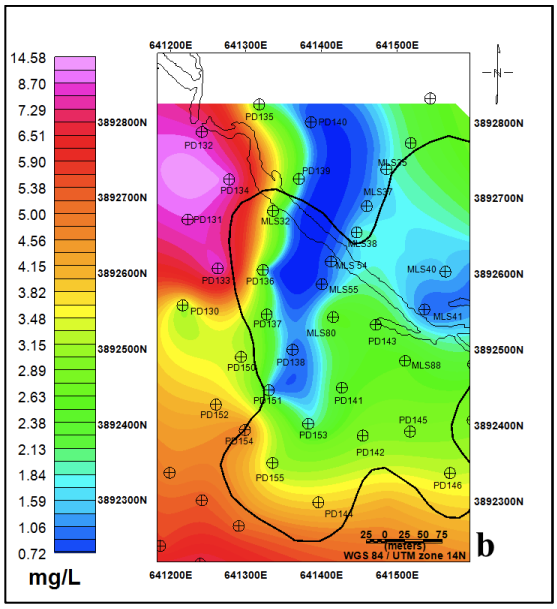

Figure 5.b Sulfate distribution map at deep depth

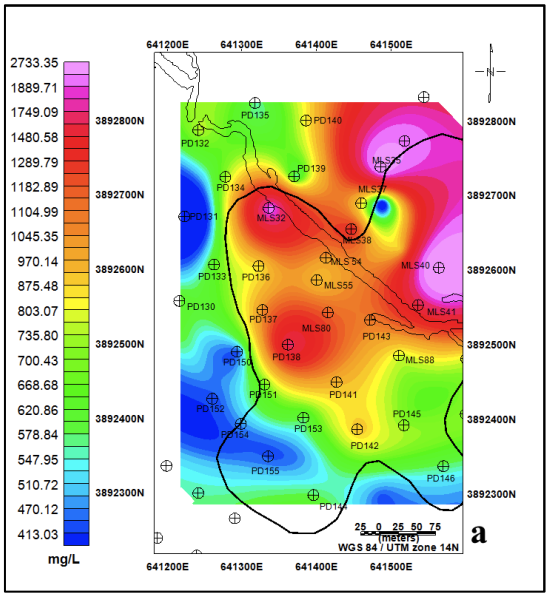

Figure 6.a Bicarbonate (HCO_3^-) distribution map at shallow depth

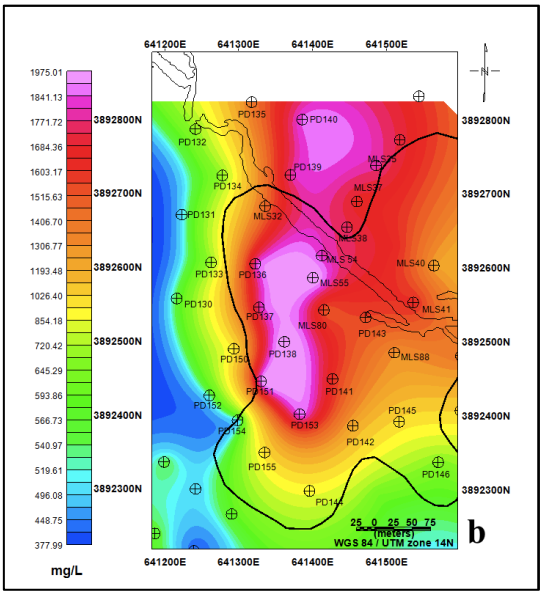

Figure 6.bBicarbonate (HCO_3^-) distribution map at deepdepth

VITA

Sen Wei

Candidate for the Degree of

Master of Science

Thesis: INVESTIGATING THE BIOGEOBATTERY MODEL FOR FIELD SPONTANEOUS POTENTIAL (SP) SIGNATURES OVER AN ORGANIC RICH PLUME AT THE NORMAN LANDFILL, OK

Major Field: Geology

Biographical:

Personal: Born in Liaoning, China, December 4th 1986 to Mr and Mrs. Zuocai and Guiling Wei.

Education:

Graduated high school from Jinzhou High Middle in July 2005.

Attended Liaoning Technical University in Fuxin, Liaoning China between August 2005 and May 2009 and graduated with a Bachelors in Geology.

Attended Oklahoma State University in Stillwater Oklahoma between August 2009 and December 2012 and completed the requirements for the Master of Science in Geology.

Experience: Employed by the Boone Pickens school of Geology as a research assistant. (Spring 2011~ Spring 2012).

Professional Memberships:

American Association of Petroleum Geologists (AAPG)

Society of Exploration Geophysicists (SEG)

American Geophysicists Untion (AGU)